Tacrolimus suppresses glucose-induced insulin release from pancreatic islets by reducing glucokinase activity

Razvan Gheorghe Radu,[1] Shimpei Fujimoto,[1] Eri Mukai,[1] Mihoko Takehiro,[1] Dai Shimono,[1]
Koichiro Nabe,[1] Makiko Shimodahira,[1] Rieko Kominato,[1] Yo Aramaki,[1] Yuichi Nishi,[1]
Shogo Funakoshi,[1] Yuichiro Yamada,[1] and Yutaka Seino[1,2]

[1]*Department of Diabetes and Clinical Nutrition, Graduate School of Medicine,
Kyoto University, Kyoto; and* [2]*Kansai-Denryoku Hospital, Osaka, Japan*

Radu, Razvan Gheorghe, Shimpei Fujimoto, Eri Mukai, Mi-
hoko Takehiro, Dai Shimono, Koichiro Nabe, Makiko Shimoda-
hira, Rieko Kominato, Yo Aramaki, Yuichi Nishi, Shogo Funa-
koshi, Yuichiro Yamada, and Yutaka Seino. Tacrolimus suppresses
glucose-induced insulin release from pancreatic islets by reducing
glucokinase activity. *Am J Physiol Endocrinol Metab* 288: E365–
E371, 2005. First published October 12, 2004; doi:10.1152/
ajpendo.00390.2004.—Tacrolimus is widely used for immunosup-
pressant therapy, including various organ transplantations. One of its
main side effects is hyperglycemia due to reduced insulin secretion,
but the mechanism remains unknown. We have investigated the
metabolic effects of tacrolimus on insulin secretion at a concentration
that does not influence insulin content. Twenty-four-hour exposure to
3 nM tacrolimus reduced high glucose (16.7 mM)-induced insulin
secretion (control 2.14 $\pm$ 0.08 vs. tacrolimus 1.75 $\pm$ 0.02
ng·islet^{-1}·30 min^{-1}, $P < 0.01$) without affecting insulin content. In
dynamic experiments, insulin secretion and NAD(P)H fluorescence
during a 20-min period after 10 min of high-glucose exposure were
reduced in tacrolimus-treated islets. ATP content and glucose utiliza-
tion of tacrolimus-treated islets in the presence of 16.7 mM glucose
were less than in control (ATP content: control 9.69 $\pm$ 0.99 vs.
tacrolimus 6.52 $\pm$ 0.40 pmol/islet, $P < 0.01$; glucose utilization:
control 103.8 $\pm$ 6.9 vs. tacrolimus 74.4 $\pm$ 5.1 pmol·islet^{-1}·90
min^{-1}, $P < 0.01$). However, insulin release from tacrolimus-treated
islets was similar to that from control islets in the presence of 16.7
mM α-ketoisocaproate, a mitochondrial fuel. Glucokinase activity,
which determines glycolytic velocity, was reduced by tacrolimus
treatment (control 65.3 $\pm$ 3.4 vs. tacrolimus 49.9 $\pm$ 2.8
pmol·islet^{-1}·60 min^{-1}, $P < 0.01$), whereas hexokinase activity was
not affected. These results indicate that glucose-stimulated insulin
release is decreased by chronic exposure to tacrolimus due to reduced
ATP production and glycolysis derived from reduced glucokinase
activity.

islet; adenosine 5′-triphosphate

TACROLIMUS (FK-506) IS AN IMMUNOSUPPRESSANT widely used in
human organ transplantation. Immunosuppression by the agent is
due to blocking of antigen-stimulated expression of genes, includ-
ing interleukin-2 in T lymphocytes, which is required for T-cell
proliferation (34). Interleukin-2 gene transcription is activated by
dephosphorylation and nuclear translocation of a transcriptional
cofactor, the nuclear factor of activated T cells (NFAT). Tacroli-
mus binds specific intracellular proteins, FK-506-binding proteins
(FKBPs), and inhibits calcineurin (protein phosphatase-2B), a
Ca^{2+}/calmodulin-dependent Ser/Thr phosphatase (7, 28) that de-
phosphorylates and translocates NFAT to nuclei (20, 37). Thus
tacrolimus suppresses interleukin-2 gene transcription by inhibit-
ing the calcineurin/NFAT pathway.

The main adverse reaction in tacrolimus-treated patients is
hyperglycemia due to reduced insulin release (6, 16, 26). The
mechanism of the inhibitory effect of tacrolimus on insulin
release has been described. Tacrolimus markedly reduces the
number of endocrine secretory granules in human pancreatic
β-cells, which correlates with the blood concentration of the
agent and is reversible by reduction of the dose (5, 15). The
agent decreases insulin release, insulin content, and insulin
mRNA concentration dependently in experiments using cell
lines, rat islets, and human islets (27, 30, 31, 32). Tacrolimus
also suppresses insulin gene expression, which is induced by
intracellular Ca^{2+} elevation via the calcineurin/NFAT pathway
(17). Thus reduced insulin content due to reduced insulin
synthesis plays an important role in the inhibitory effect of
tacrolimus on insulin release.

The mechanism of glucose-stimulated insulin release from
pancreatic β-cells has been well documented. Glucose stimu-
lates insulin secretion by both triggering and amplifying sig-
nals in pancreatic β-cells (14). The triggering pathway includes
entry of glucose into β-cells, acceleration of glycolysis in
cytosol and glucose oxidation in mitochondria, an increase in
ATP content and ATP-to-ADP ratio, closure of ATP-sensitive
K^+ (K_{ATP}) channels, membrane depolarization, opening of
voltage-dependent Ca^{2+} channels (VDCCs), an increase in
Ca^{2+} influx through VDCCs, raised intracellular Ca^{2+} concen-
tration ($[Ca^{2+}]_i$), and exocytosis of insulin granules. It has been
reported that glucose also enhances insulin secretion K_{ATP}
channel independently. The K_{ATP} channel-independent ampli-
fying action of glucose has been confirmed by treatment of
β-cells with diazoxide, which prevents K_{ATP} channels from
closing, and with a depolarizing concentration of extracellular
K^+ that restores Ca^{2+} influx (1, 12). Because glucose does not
increase $[Ca^{2+}]_i$ but nevertheless augments insulin release
under these conditions, glucose may well exert its effects by
increasing Ca^{2+} efficacy in stimulation-secretion coupling, due
at least in part to the direct effect of increased ATP derived
from glucose metabolism on exocytosis (14). Thus glucose
metabolism in β-cells plays a crucial role in glucose-induced
insulin release. However, the effect of tacrolimus on glucose-
induced insulin release and glucose metabolism has not been
examined in detail.

Address for reprint requests and other correspondence: S. Fujimoto, Dept. of
Diabetes and Clinical Nutrition, Graduate School of Medicine, Kyoto Univ.,
54 Shogoin Kawahara-cho, Sakyo-ku, Kyoto 606-8507, Japan (E-mail:
fujimoto@metab.kuhp.kyoto-u.ac.jp).

We have investigated the effects of chronic exposure to tacrolimus on insulin release by functional analysis of the metabolic responses of tacrolimus-treated islets.

MATERIALS AND METHODS

Materials. Tacrolimus (FK-506) was donated by Fujisawa Pharmaceutical (Tokyo, Japan). RPMI 1640 and glucose-6-phosphate dehydrogenase (G6PDH) were obtained from Sigma (St. Louis, MO). Luciferin-luciferase was obtained from Turner Designs (Sunnyvale, CA). ^3H_2O and [5-^3H]glucose were obtained from Amersham (Buckinghamshire, UK). All other agents were obtained from Nacalai Tesque (Kyoto, Japan).

Animals. Male Wistar rats weighing 180–230 g were obtained from Shimizu (Kyoto, Japan). The animals were fed standard lab chow ad libitum and allowed free access to water in an air-conditioned room with a 12:12-h light-dark cycle until the experiments. All experiments were carried out with rats aged 8–12 wk. The animals were maintained and used in accordance with the Guidelines for Animal Experiments of Kyoto University.

Islet isolation and culture. Islets of Langerhans were isolated from Wistar rats by collagenase digestion, as described previously (8). Isolated islets were cultured for 24 h in RPMI 1640 medium containing 10% FCS, 100 U/ml penicillin, 100 μg/ml streptomycin, and 5.5 mM glucose with or without tacrolimus at 37°C in humidified air containing 5% CO_2.

Measurement of insulin release from isolated rat pancreatic islets. Insulin release from intact islets was monitored using either batch incubation or a perifusion system described previously, using Krebs-Ringer bicarbonate buffer (KRBB) supplemented with 0.2% bovine serum albumin (BSA; fraction V) and 10 mM HEPES, adjusted to pH 7.4 (KRBB medium) (8).

For static incubation experiments, cultured islets were preincubated at 37°C for 30 min in KRBB medium supplemented with 2.8 mM glucose. Groups of five islets were then batch incubated for 30 min in 0.7 ml of KRBB medium with test materials. At the end of the incubation period, the islets were pelleted by centrifugation, and aliquots of the buffer were sampled.

For perifusion experiments, groups of 20 cultured islets were placed in each of the parallel chambers of a perifusion apparatus and perifused with KRBB medium at a rate of 0.7 ml/min at 37°C. The medium was continuously gassed with 95% O_2-5% CO_2. The islets were perifused for 30 min to establish a stable insulin secretory rate at a basal level of glucose and then exposed to the stimulating levels of glucose. The amount of immunoreactive insulin was determined by RIA with rat insulin as standard.

Measurement of insulin and DNA content. Insulin contents and DNA contents of islets were measured as previously described (10). Briefly, after an aliquot of incubation medium for insulin release assay was taken, the islets remaining were lysed. Insulin content was determined by RIA using diluted samples. DNA content was determined by fluorometric assay using bisbenzimidazole (Hoechst 33258) as fluorochrome and calf thymus DNA (type I, Sigma) as standard.

Measurement of NAD(P)H fluorescence. Cultured islets without dye were immediately placed in a heat-controlled chamber on the stage of an inverted microscope kept at 36 ± 1°C and superfused with KRBB medium with 2.8 mM glucose for 30 min. The islets were excited successively at 360 nm, and the fluorescence emitted at 470 nm (13) was captured every 20 s by a charge-coupled device camera (Micro Max 5-MHz System; Roper Industries, Trenton, NJ). Changes in NAD(P)H fluorescence signal were expressed as percent control values by dividing the signal at a given time by the average signal at 2.8 mM glucose during the last 5 min before stimulation. Images of NAD(P)H were analyzed with the Meta Fluor image analyzing system (Universal Imaging, West Chester, PA).

Measurement of ATP content. ATP contents were determined as previously described, with a slight modification (10). Briefly, after groups of cultured islets were preincubated at 2.8 mM glucose for 30 min, groups of 15 islets were batch incubated in 0.5 ml of KRBB medium containing 2.8 or 16.7 mM glucose at 37°C for 30 min. Incubation was stopped by the addition of 0.1 ml of 2 M $HClO_4$. The tubes were immediately mixed with vortex and sonicated in ice-cold water. They were then centrifuged, and a fraction (0.4 ml) of the supernatant was mixed with 0.1 ml of 2 M HEPES and 0.1 ml of 1 M Na_2CO_3. The ATP concentration was measured by adding 0.2 ml of luciferin-luciferase solution to a fraction sample (0.1 ml) in a bioluminometer (Luminometer model 20e; Turner Designs). To draw a standard curve, blanks and ATP standards were run through the entire procedure, including the extraction steps.

Measurement of glucose utilization. Glucose utilization was measured, using a previously described method (2) with a slight modification. Cultured islets were preincubated in KRBB medium with 2.8 mM glucose at 37°C for 30 min. Batches of 30 islets for each condition were incubated at 37°C for 90 min in 150 μl of medium containing 1.5 μCi of [5-^3H]glucose. Aliquots of the incubation medium (100 μl) and 20 μl of 1 M HCl were transferred into small tubes and placed into a glass vial containing 0.5 ml of H_2O. The capped vials were incubated overnight at 37°C to vaporize ^3H_2O from the solution. The inner tube was then lifted out, and the disintegrations per minute of water-melting ^3H_2O in the vial were counted. In a parallel incubation, the recovery ratio of ^3H_2O was measured using ^3H_2O. After subtracting blank disintegrations per minute from sample disintegrations per minute, glucose utilization was calculated using the disintegrations per minute, specific radioactivity of [5-^3H]glucose, and recovery ratio of ^3H_2O.

Measurement of glucokinase and hexokinase activity. Glucokinase activity was measured by a fluorometric assay according to a method reported previously (25, 38). After cultured islets were preincubated with KRBB medium with 2.8 mM glucose, 100 islets were homogenized in 250 μl of solution containing 20 mM KH_2PO_4, 100 mM KCl, 1 mM $MgCl_2$, 1 mM EDTA, 5% glycerol, and 1 mM DTT (pH 7 by KOH), and the supernatants (islet extracts) were obtained from the homogenates by centrifugation (10,000 g, 15 min) at 4°C. The glucose phosphorylation rate was estimated as the increase in NADH through the following reaction: glucose-6-phosphate + NAD → 6-phospho-glucono-δ-lactone + NADH by NAD-dependent G6PDH. The enzyme reaction was performed using 25 μl of islet extracts in a 160-μl solution consisting of 50 mM HEPES (pH 7.4 by NaOH), 100 mM KCl, 8 mM $MgCl_2$, 0.5 mM NAD, 5 mM ATP, 1 mM DTT, and 1 U/ml G-6-PDH supplemented with two concentrations (50 mM and 0.5 mM) of glucose at 37°C for 1 h; it was stopped by adding 290 μl of stopping solution (300 mM Na_2HPO_4, 0.46 mM SDS, pH 8.0). NADH concentration was measured by fluorometry (Shimazu RF-5000, Kyoto, Japan) at a 340-nm excitation and a 450-nm emission. Blanks in the absence of ATP were incubated in a parallel experiment and were subtracted from the total fluorescence of the corresponding complete reaction mixtures. Glucokinase activity was determined by subtracting hexokinase activity measured at 0.5 mM glucose from the activity measured at 50 mM glucose.

Statistical analysis. Results are expressed as means ± SE. Statistical significance was evaluated by unpaired Student's t-test. $P < 0.05$ was considered significant.

RESULTS

Effect of chronic exposure to tacrolimus on glucose-induced insulin release, insulin content, and DNA content in islets. Chronic (24 h) exposure to tacrolimus (3–30 nM) concentrations dependently suppressed 16.7 mM glucose-induced insulin release but did not affect basal insulin release in the presence of 2.8 mM glucose (Table 1). Insulin content was significantly reduced by 24-h exposure to 10 and 30 nM tacrolimus (Table 2). However, 24-h exposure to 3 nM tacroli-

- 40 -

Table 1. *Concentration-dependent effect of chronic exposure to tacrolimus on glucose-induced insulin release from pancreatic islets*

Experimental Condition During Culture	Insulin Release, ng·islet^{-1}·30 min^{-1}	
	Basal (2.8 mM glucose)	Stimulated (16.7 mM glucose)
Control	0.26±0.02	2.14±0.08
3 nM Tacrolimus	0.26±0.03	1.75±0.02*
10 nM Tacrolimus	0.24±0.02	1.53±0.04*
30 nM Tacrolimus	0.21±0.02	1.49±0.03*

Values represent means ± SE of 16 determinations from several experiments. Islets were cultured under the conditions indicated for 24 h. After cultured islets were preincubated with 2.8 mM glucose for 30 min, insulin release in the presence of 2.8 and 16.7 mM glucose for 30 min was determined. *$P < 0.01$ vs. control (cultured without tacrolimus).

mus significantly suppressed high glucose-induced insulin release but did not affect insulin content (Tables 1 and 2). DNA content was not altered by 24-h exposure to 3, 10, and 30 nM tacrolimus, indicating that these concentrations of tacrolimus do not reduce islet mass (Table 2). Accordingly, islets cultured with 3 nM tacrolimus for 24 h were used to investigate the reduction in glucose-induced insulin release without the influence of altered insulin content. In perifusion experiments, basal insulin release was similar in control and tacrolimus-treated islets (Fig. 1A). High glucose-induced biphasic insulin release from tacrolimus-treated islets was reduced compared with control islets after 10 min of high-glucose exposure (Fig. 1A). Mean insulin release during the first 10 min after high-glucose exposure was not affected, whereas that during the second and third 10-min period was suppressed in tacrolimus-treated islets (mean insulin release from 20 to 30 min: tacrolimus 0.60 ± 0.03 vs. control 0.86 ± 0.06 ng·10 islets^{-1}·min^{-1}, $n = 6$, $P < 0.01$; Fig. 1B). Exposure (12 h) to 3 nM tacrolimus inhibited high glucose-induced insulin release to the level brought about by 24-h exposure. However, the inhibitory effect of 12-h exposure to 3 nM tacrolimus was almost completely recovered by the withdrawal of tacrolimus for 12 h (Table 3).

Effect of chronic exposure to tacrolimus on α-ketoisocaproate-induced insulin release. Inhibitors of glycolysis, including mannoheptulose (20 mM) and iodoacetate (1 mM), almost completely suppressed glucose-induced insulin release but did not affect α-ketoisocaproate (KIC)-induced insulin release (Table 4). These results indicate that KIC-induced insulin release is not affected by inhibition of glycolysis. To characterize metabolic fuel-induced insulin release independent of the inhibition of glycolysis, KIC-induced insulin release from ta-

Table 2. *Effect of chronic exposure to tacrolimus on insulin content and DNA content*

Experimental Condition During Culture	Insulin Content, ng/islet	DNA Content, ng/islet
Control	25.0±0.7	19.3±0.7
3 nM Tacrolimus	26.2±1.0	21.1±0.8
10 nM Tacrolimus	22.4±1.1*	20.1±1.0
30 nM Tacrolimus	20.4±0.8*	19.9±1.0

Values represent means ± SE of 16 determinations from several experiments. At the end of the experiments indicated in Table 1, insulin content and DNA content were determined, using islets in a randomly selected half of the batches. *$P < 0.01$ vs. control (cultured without tacrolimus).
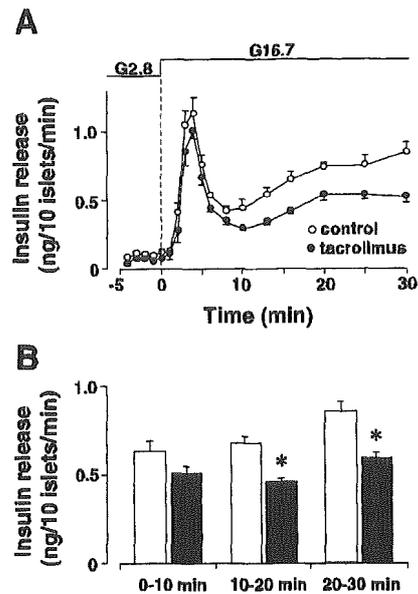

Fig. 1. High (16.7 mM) glucose-induced biphasic insulin release in control and tacrolimus-treated islets. Islets were cultured with or without 3 nM tacrolimus for 24 h. After cultured islets were perifused with 2.8 mM glucose (G2.8) for 30 min, they were stimulated with 16.7 mM glucose (G16.7) at *time 0* for 30 min. A: time course of high glucose-induced biphasic insulin release in control and tacrolimus-treated islets. Values represent means ± SE of 6 determinations. All values in tacrolimus-treated islets after 10 min of exposure to high glucose were significantly less than the corresponding values in control ($P < 0.01$). B: average values calculated from the data in A. Average values during indicated time period after high-glucose exposure in control (open bar) and tacrolimus-treated islets (solid bar) are shown. *$P < 0.01$ vs. corresponding control.

crolimus-treated islets was examined. Chronic exposure to 3 nM tacrolimus did not affect KIC (16.7 mM)-induced insulin release (Table 5).

Time course of NAD(P)H fluorescence in islets. NAD(P)H fluorescence began to elevate immediately after exposure to

Table 3. *Reversible effect of tacrolimus on glucose-induced insulin release from islets*

Experimental Condition During Culture	Insulin Release, ng·islet^{-1}·30 min^{-1}	
	Basal (2.8 mM glucose)	Stimulated (16.7 mM glucose)
Control (24-h no tacrolimus)	0.26±0.02	2.15±0.09
24-h Tacrolimus	0.26±0.02	1.65±0.06*
12-h No tacrolimus + 12-h tacrolimus	0.24±0.01	1.72±0.07*
12-h Tacrolimus + 12-h no tacrolimus	0.28±0.03	2.24±0.09†

Values represent means ± SE of 8 determinations from several experiments. Two groups of islets were cultured with or without 3 nM tacrolimus for 24 h (control and 24-h tacrolimus group). One group of islets was cultured without tacrolimus for the first 12 h and with 30 nM tacrolimus for the second 12 h (12-h no tacrolimus + 12-h tacrolimus group). Another group of islets was cultured with 30 nM tacrolimus for the first 12 h and without tacrolimus for the second 12 h (12-h tacrolimus, + 12-h no tacrolimus group). After cultured islets were preincubated with 2.8 mM glucose for 30 min, insulin release in the presence of 2.8 and 16.7 mM glucose for 30 min was determined. *$P < 0.01$ vs. control (24-h no tacrolimus). †$P < 0.01$ vs. 24-h tacrolimus. Stimulated insulin release was not different between 24-h tacrolimus and 12-h no tacrolimus + 12-h tacrolimus and between control (24-h no tacrolimus) and 12-h tacrolimus + 12-h no tacrolimus.

Table 4. *Effect of glycolytic inhibition on glucose-induced and KIC-induced insulin release from pancreatic islets*

| | Insulin Release, ng·islet^{-1}·30 min^{-1} | | | |
| | Glucose | | KIC | |
Experimental Condition	2.8 mM	16.7 mM	2.8 mM	16.7 mM
Control	0.25±0.01	2.15±0.10	0.25±0.04	1.91±0.09
20 mM Mannoheptulose	0.22±0.03	0.24±0.02*	0.24±0.02	1.99±0.13
1 mM Iodoacetate	0.22±0.01	0.27±0.02*	0.23±0.01	2.02±0.08

Values represent means ± SE of 16 determinations from several experiments. Islets were cultured without tacrolimus for 24 h. After cultured islets were preincubated with 2.8 mM glucose for 30 min, insulin release in the presence of 2.8 and 16.7 mM glucose or α-ketoisocaproate (KIC) for 30 min with or without glycolytic inhibitors was determined. *$P < 0.01$ vs. control (16.7 mM glucose without inhibitors).

high glucose in both groups of islets and reached a plateau within 10 min after exposure (Fig. 2A). A significant attenuation of NAD(P)H fluorescence was observed from 10 min in tacrolimus-cultured islets (at 10 min: tacrolimus 124.9 ± 1.3, $n = 11$, vs. control $129.3 \pm 1.1\%$, $n = 12$, $P < 0.05$; Fig. 2A). Mean NAD(P)H fluorescence during the first 10 min after high-glucose exposure was not affected, whereas that during the second and third 10-min period was suppressed in tacrolimus-treated islets [mean NAD(P)H fluorescence from 20 to 30 min: tacrolimus 124.5 ± 1.2, $n = 11$, vs. control $133.9 \pm 1.4\%$, $n = 12$, $P < 0.01$; Fig. 2B].

Effect of tacrolimus on ATP content. ATP content was greater in islets incubated with 16.7 mM glucose than in islets incubated with 2.8 mM glucose in both control (2.8 mM glucose, 5.22 ± 0.51, vs. 16.7 mM glucose, 9.69 ± 0.99 pmol/islet, $n = 10$, $P < 0.01$) and tacrolimus-treated islets (2.8 mM glucose, 4.75 ± 0.50, vs. 16.7 mM glucose, 6.52 ± 0.40 pmol/islet, $n = 10$, $P < 0.05$). ATP content in the presence of 16.7 mM glucose was significantly reduced in tacrolimus-treated islets ($P < 0.01$) but in the presence of 2.8 mM glucose was not affected by tacrolimus (Fig. 3A).

Effect of tacrolimus on glucose utilization. Glucose utilization was greater in islets incubated with 16.7 mM glucose than in islets incubated with 2.8 mM glucose in both control (2.8 mM glucose, 35.1 ± 6.1, vs. 16.7 mM glucose, 103.8 ± 6.9 pmol·islet^{-1}·90 min^{-1}, $n = 9$, $P < 0.01$) and tacrolimus-treated islets (2.8 mM glucose, 24.6 ± 3.7, vs. 16.7 mM glucose, 73.4 ± 5.1 pmol·islet^{-1}·90 min^{-1}, $n = 9$, $P < 0.01$). Glucose utilization in the presence of 16.7 mM glucose was significantly reduced in tacrolimus-treated islets ($P < 0.01$) but

Table 5. *Effect of chronic exposure to tacrolimus on KIC-induced insulin release from pancreatic islets*

| | Insulin Release, ng·islet^{-1}·30 min^{-1} | |
Experimental Condition During Culture	Basal (2.8 mM KIC)	Stimulated (16.7 mM KIC)
Control	0.28±0.02	2.09±0.04
3 nM Tacrolimus	0.23±0.02	2.05±0.04

Values represent means ± SE of 16 determinations from several experiments. Islets were cultured under the conditions indicated for 24 h. After cultured islets were preincubated with 2.8 mM glucose for 30 min, insulin release in the presence of 2.8 and 16.7 mM KIC for 30 min was determined.
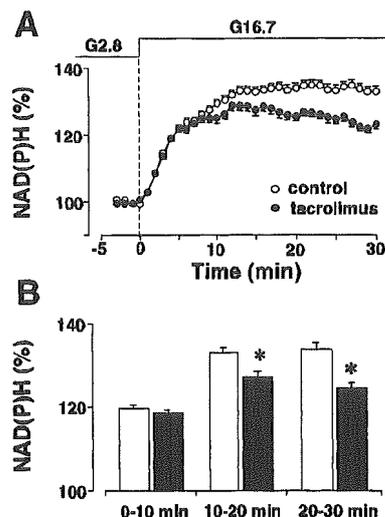

Fig. 2. High (16.7 mM) glucose-induced NAD(P)H fluorescence elevation in control and tacrolimus-treated islets. Islets were cultured with or without 3 nM tacrolimus for 24 h. After cultured islets were perifused with 2.8 mM glucose for 30 min, they were stimulated with 16.7 mM glucose at *time 0* for 30 min. *A*: time course of high glucose-induced NAD(P)H fluorescence elevation in control and tacrolimus-treated islets. Values represent means ± SE of 12 (control) or 11 (tacrolimus) determinations from the several experiments. All values, except those at 12 min, in tacrolimus-treated islets after 10 min of exposure to high glucose were significantly less than the corresponding values in control (at 10, 11, 13, 14, 15, and 16 min: $P < 0.05$; after 17 min: $P < 0.01$). *B*: average values calculated from the data in *A*. Average values during indicated time period after high-glucose exposure in control (open bar) and tacrolimus-treated islets (solid bar) are shown. *$P < 0.01$ vs. corresponding control.

in the presence of 2.8 mM glucose was not affected by tacrolimus (Fig. 3B).

Effect of tacrolimus on glucokinase and hexokinase activity. Glucokinase activity was significantly decreased by the tacrolimus treatment (tacrolimus 49.9 ± 3.4 vs. control 65.3 ± 3.4 pmol·islet^{-1}·60 min^{-1}, $n = 10$, $P < 0.01$), whereas hexokinase activity was not affected (tacrolimus 35.5 ± 2.8 vs. control 34.1 ± 2.1 pmol·islet^{-1}·60 min^{-1}, $n = 10$, not significant; Fig. 3C).

DISCUSSION

In the present study, we show that a low concentration of tacrolimus suppresses high glucose-induced insulin secretion from pancreatic islets without affecting insulin content. This inhibitory effect of tacrolimus is the result of reduced ATP production and glycolysis due to decreased glucokinase activity.

We found that 3 nM tacrolimus, a lower concentration than used in previous reports (31, 32, 41), significantly decreased glucose-induced insulin release after 24-h exposure without affecting insulin content, which indicates that reduced insulin release by tacrolimus is not necessarily derived from reduced insulin content. To investigate the mechanism of reduced insulin release by tacrolimus independent of reduced insulin content, we used 3 nM tacrolimus-treated islets. Recommended trough concentrations of tacrolimus in blood are 3–6 ng/ml (3.6–7.2 nM) and 5–15 ng/ml (6.1–18.2 nM) in islet transplantation (36) and in liver transplantation (3), respectively. Ac-
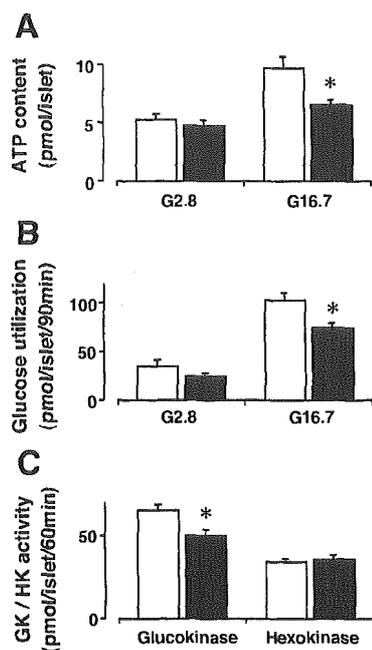
- 42 -

A

B

C

Fig. 3. Metabolic parameters in control (open bars) and tacrolimus-treated islets (solid bars). Islets were cultured with or without 3 nM tacrolimus for 24 h. Cultured islets were preincubated with 2.8 mM glucose for 30 min. *A*: ATP content. After preincubation, islets were incubated in the presence of 2.8 or 16.7 mM glucose. Values represent means ± SE of 10 determinations from several experiments. *B*: glucose utilization. After preincubation, islets were incubated in the presence of 2.8 or 16.7 mM glucose. Values represent means ± SE of 9 determinations from several experiments. *C*: glucokinase (GK) and hexokinase (HK) activities. Values represent means ± SE of 10 determinations from several experiments. *$P < 0.01$ vs. corresponding control.

cordingly, the concentration used in our experiments is comparable to clinically used concentrations.

Chronic exposure to 1 μM tacrolimus for 7 days has been shown not to alter the extent of islet cell apoptosis or necrosis (41), suggesting that apoptosis and necrosis in islets are not increased in our experimental condition. In addition, the inhibitory effect of chronic exposure to 3 nM tacrolimus was almost completely recovered by withdrawal of tacrolimus. For these reasons, the reduced glucose-induced insulin release from 3 nM tacrolimus-treated islets is unlikely to be derived from nonspecific irreversible toxic effects of the agent.

In dynamic experiments, both glucose-induced biphasic insulin release and glucose-induced elevation of NAD(P)H fluorescence were reduced by tacrolimus treatment after 10 min of glucose exposure, suggesting that the reduced insulin release results from reduced glucose metabolism. Accordingly, ATP, the most important metabolic signal in insulin release, was investigated. Because insulin content per islet was not different between control and tacrolimus-treated islets in the present study, the sizes of the stable pool of ATP in an islet, which occurs mainly in the insulin granules, and the diffusible pool, which occurs mainly in the cytosol (4), were not very different. Therefore, the comparison of total ATP content is valid. ATP content in the presence of high glucose was reduced in tacrolimus-treated islets. Mitochondrial ATP production is driven by the H^+ gradient across the mitochondrial membrane generated by transport of high-energy elec-

trons in the respiratory chain. These electrons are derived from NADH and $FADH_2$, which are derived from the TCA cycle in the matrix and/or transferred from the cytosol by the shuttle system. A reduced supply of substrates to mitochondria results in a decreased H^+ gradient across the mitochondrial membrane. Glucose utilization reflects the velocity of glycolysis (24), and NAD(P)H autofluorescence dominantly reflects the redox state of mitochondria (29). Because both glucose utilization and NAD(P)H fluorescence in the presence of high glucose were decreased in tacrolimus-treated islets, the reduced ATP content in these islets may well be attributable to a decreased supply of reduced equivalents to mitochondria.

In pancreatic islets, KIC is oxidized, enhancing ATP production and triggering insulin release (21). However, the mechanism of KIC-induced insulin release is not fully understood, and two distinct mechanisms are proposed. First, KIC, which is converted to acetyl-CoA via a branched-chain α-ketoacid dehydrogenase (BCKDH)-dependent pathway, enters into the TCA cycle and is oxidized (18, 19). Second, KIC, together with endogenous glutamate, is converted to α-ketoglutarate via glutamate-ketoacid transaminase (GKAT), which enters into the TCA cycle and is oxidized (11). Because both BCKDH and GKAT are mitochondrial enzymes, KIC should be metabolized within mitochondria without affecting cytosolic glycolysis. Our results show that mannoheptulose, a glucokinase inhibitor (39), and iodoacetate, a glyceraldehyde-3-phosphate dehydrogenase inhibitor (35), both of which inhibit glycolysis, decreased glucose-induced insulin release but did not affect KIC-induced insulin release. These results are compatible with the notion that KIC is metabolized within mitochondria without affecting cytosolic glycolysis. Accordingly, KIC-induced insulin release was examined to clarify the effect of tacrolimus on mitochondrial metabolism independent of glycolysis. Because tacrolimus reduced glucose-induced insulin release but did not affect KIC-induced insulin release, the decreased glucose metabolism should be derived from reduced glycolysis.

Glucokinase is a rate-limiting enzyme in glycolysis and serves as glucose sensor in pancreatic β-cells (22). Regulation of the enzyme has a central impact on β-cell function, as demonstrated in studies of glucokinase mutations identified in patients with maturity onset diabetes of the young (42). The activity of the enzyme is reduced in tacrolimus-treated islets and presumably plays a primary role in reducing glucose-induced insulin release without a decrease in insulin content by the agent.

Recently, Uchizono et al. (41) reported an effect of chronic exposure to tacrolimus (mainly 100 nM) on the mechanism of insulin release under reduced insulin content. Interestingly, glucose-induced insulin release was found to be more profoundly suppressed than mitochondrial fuel-induced insulin release, a phenomenon clarified by our results. They assert that tacrolimus impairs glucose-induced insulin release and has effects distal to the rise in intracellular Ca^{2+}, which could be explained by a reduced ATP level by the agent, as ATP directly enhances Ca^{2+} efficacy in the exocytotic system of insulin release (9, 33, 40).

Glucokinase activity in pancreatic β-cells is regulated on both translational and posttranslational levels, but the mechanism remains largely unknown (23). Further investigation of suppression of glucokinase activity by tacrolimus may clarify the regulation of glucokinase activity in pancreatic β-cells.

REFERENCES

1. **Aizawa T, Komatsu M, Asanuma N, Sato Y, and Sharp GWG.** Glucose action "beyond ionic events" in the pancreatic β cell. *Trends Pharmacol Sci* 19: 496–499, 1998.
2. **Ashcroft SJ, Weerasinghe LC, Bassett JM, and Randle PJ.** The pentose cycle and insulin release in mouse pancreatic islets. *Biochem J* 126: 525–532, 1972.
3. **Busuttil RW and Lake JR.** Role of tacrolimus in the evolution of liver transplantation. *Transplantation* 77: S44–S51, 2004.
4. **Detimary P, Jonas JC, and Henquin JC.** Stable and diffusible pools of nucleotides in pancreatic islet cells. *Endocrinology* 137: 4671–4676, 1996.
5. **Drachenberg CB, Klassen DK, Weir MR, Wiland A, Fink JC, Bartlett ST, Cangro CB, Blahut S, and Papadimitriou JC.** Islet cell damage associated with tacrolimus and cyclosporine: morphological features in pancreas allograft biopsies and clinical correlation. *Transplantation* 68: 396–402, 1999.
6. **Filler G, Neuschulz I, Vollmer I, Amendt P, and Hocher B.** Tacrolimus reversibly reduces insulin secretion in paediatric renal transplant recipients. *Nephrol Dial Transplant* 15: 867–871, 2000.
7. **Fruman DA, Klee CB, Bierer BE, and Burakoff SJ.** Calcineurin phosphatase activity in T lymphocytes is inhibited by FK 506 and cyclosporin A. *Proc Natl Acad Sci USA* 89: 3686–3690, 1992.
8. **Fujimoto S, Ishida H, Kato S, Okamoto Y, Tsuji K, Mizuno N, Ueda S, Mukai E, and Seino Y.** The novel insulinotropic mechanism of pimobendan: direct enhancement of the exocytotic process of insulin secretory granules by increased Ca^{2+} sensitivity in β-cells. *Endocrinology* 139: 1133–1140, 1998.
9. **Fujimoto S, Mukai E, Hamamoto Y, Takeda T, Takehiro M, Yamada Y, and Seino Y.** Prior exposure to high glucose augments depolarization-induced insulin release by mitigating the decline of ATP level in rat islets. *Endocrinology* 143: 213–221, 2002.
10. **Fujimoto S, Tsuura Y, Ishida H, Tsuji K, Mukai E, Kajikawa M, Hamamoto Y, Takeda T, Yamada Y, and Seino Y.** Augmentation of basal insulin release from rat islets by preexposure to a high concentration of glucose. *Am J Physiol Endocrinol Metab* 279: E927–E940, 2000.
11. **Gao Z, Young RA, Li G, Najafi H, Buettger C, Sukumvanich SS, Wong RK, Wolf BA, and Matschinsky FM.** Distinguishing features of leucine and α-ketoisocaproate sensing in pancreatic β-cells. *Endocrinology* 144: 1949–1957, 2003.
12. **Gembal M, Gilon P, and Henquin JC.** Evidence that glucose can control insulin release independently from its action on ATP-sensitive K^+ channels in mouse B cells. *J Clin Invest* 89: 1288–1295, 1992.
13. **Gilon P and Henquin JC.** Influence of membrane potential changes on cytoplasmic Ca^{2+} concentration in an electrically excitable cell, the insulin-secreting pancreatic B-cell. *J Biol Chem* 267: 20713–20720, 1992.
14. **Henquin JC.** Triggering and amplifying pathways of regulation of insulin secretion by glucose. *Diabetes* 49: 1751–1760, 2000.
15. **Hirano Y, Fujihira S, Ohara K, Katsuki S, and Noguchi H.** Morphological and functional changes of islets of Langerhans in FK-506-treated rats. *Transplantation* 53: 889–894, 1992.
16. **Jain AB, Fung JJ, Todo S, Reyes J, Selby R, Irish W, Doyle H, Abu-Elmagd K, Casavilla A, Nour B, Bronsther O, Jabbour N, Pinna A, Dodson F, Ramos H, McMichael JJ, McCauley J, Tzakis AG, Marino I, Marsh W, Venkataramanan R, Iwatsuki S, and Starzl TE.** One thousand consecutive primary orthotopic liver transplants under FK 506: survival and adverse events. *Transplant Proc* 27: 1099–1104, 1995.
17. **Lawrence MC, Bhatt HS, Watterson JM, and Easom RA.** Regulation of insulin gene transcription by a Ca^{2+}-responsive pathway involving calcineurin and nuclear factor of activated T cells. *Mol Endocrinol* 15: 1758–1767, 2001.
18. **Lenzen S, Formanek H, and Panten U.** Signal function of metabolism of neutral amino acids and 2-keto acids for initiation of insulin secretion. *J Biol Chem* 257: 6631–6633, 1982.
19. **Lenzen S, Schmidt W, and Panten U.** Transamination of neutral amino acids and 2-keto acids in pancreatic B-cell mitochondria. *J Biol Chem* 260: 12629–12634, 1985.
20. **Loh C, Shaw KT, Carew J, Viola JP, Luo C, Perrino BA, and Rao A.** Calcineurin binds the transcription factor NFAT1 and reversibly regulates its activity. *J Biol Chem* 271: 10884–10891, 1996.
21. **Malaisse WJ, Sener A, Malaisse-Legae F, Hutton JC, and Christophe J.** The stimulus-secretion coupling of amino acid-induced insulin release. Metabolic interaction of L-glutamine and 2-ketoisocaproate in pancreatic islets. *Biochim Biophys Acta* 677: 39–49, 1981.
22. **Matschinsky FM.** Banting Lecture 1995. A lesson in metabolic regulation inspired by the glucokinase glucose sensor paradigm. *Diabetes* 45: 223–241, 1996.
23. **Matschinsky FM.** Regulation of pancreatic β-cell glucokinase: from basics to therapeutics. *Diabetes* 51, Suppl 3: S394–S404, 2002.
24. **Meglasson MD and Matschinsky FM.** Pancreatic islet glucose metabolism and regulation of insulin secretion. *Diabetes Metab Rev* 2: 163–214, 1986.
25. **Miwa I, Mita Y, Murata T, Okuda J, Sugiura M, Hamada Y, and Chiba T.** Utility of 3-O-methyl-N-acetyl-D-glucosamine, an N-acetylglucosamine kinase inhibitor, for accurate assay of glucokinase in pancreatic islets and liver. *Enzyme Protein* 48: 135–142, 1994–1995.
26. **Montori VM, Basu A, Erwin PJ, Velosa JA, Gabriel SE, and Kudva YC.** Posttransplantation diabetes: a systematic review of the literature. *Diabetes Care* 25: 583–592, 2002.
27. **Oetjen E, Baun D, Beimesche S, Krause D, Cierny I, Blume R, Dickel C, Wehner S, and Knepel W.** Inhibition of human insulin gene transcription by the immunosuppressive drugs cyclosporin A and tacrolimus in primary, mature islets of transgenic mice. *Mol Pharmacol* 63: 1289–1295, 2003.
28. **O'Keefe SJ, Tamura J, Kincaid RL, Tocci MJ, and O'Neill EA.** FK-506- and CsA-sensitive activation of the interleukin-2 promoter by calcineurin. *Nature* 357: 692–694, 1992.
29. **Patterson GH, Knobel SM, Arkhammar P, Thastrup O, and Piston DW.** Separation of the glucose-stimulated cytoplasmic and mitochondrial NAD(P)H responses in pancreatic islet β cells. *Proc Natl Acad Sci USA* 97: 5203–5207, 2000.
30. **Paty BW, Harmon JS, Marsh CL, and Robertson RP.** Inhibitory effects of immunosuppressive drugs on insulin secretion from HIT-T15 cells and Wistar rat islets. *Transplantation* 73: 353–357, 2002.
31. **Polastri L, Galbiati F, Bertuzzi F, Fiorina P, Nano R, Gregori S, Aldrighetti L, Pozza G, Secchi A, Adorini L, and Davalli AM.** Secretory defects induced by immunosuppressive agents on human pancreatic β-cells. *Acta Diabetol* 39: 229–233, 2002.
32. **Redmon JB, Olson LK, Armstrong MB, Greene MJ, and Robertson RP.** Effects of tacrolimus (FK-506) on human insulin gene expression, insulin mRNA levels, and insulin secretion in HIT-T15 cells. *J Clin Invest* 98: 2786–2793, 1996.
33. **Rorsman P.** The pancreatic β-cell as a fuel sensor: an electrophysiologist's viewpoint. *Diabetologia* 40: 487–495, 1997.
34. **Sawada S, Suzuki G, Kawase Y, and Takaku F.** Novel immunosuppressive agent, FK-506. In vitro effects on the cloned T cell activation. *J Immunol* 139: 1797–1803, 1987.
35. **Sener A, Pipeleers DG, Levy J, and Malaisse WJ.** The stimulus-secretion coupling of glucose-induced insulin release. XXVI. Are the secretory and fuel functions of glucose dissociable by iodoacetate? *Metabolism* 27: 1505–1517, 1978.
36. **Shapiro AM, Lakey JR, Ryan EA, Korbutt GS, Toth E, Warnock GL, Kneteman NM, and Rajotte RV.** Islet transplantation in seven patients with type 1 diabetes mellitus using a glucocorticoid-free immunosuppressive regimen. *N Engl J Med* 343: 230–238, 2000.
37. **Shaw KT, Ho AM, Raghavan A, Kim J, Jain J, Park J, Sharma S, Rao A, and Hogan PG.** Immunosuppressive drugs prevent a rapid dephosphorylation of transcription factor NFAT1 in stimulated immune cells. *Proc Natl Acad Sci USA* 92: 11205–11209, 1995.
38. **Shiraishi A, Yamada Y, Tsuura Y, Fujimoto S, Tsukiyama K, Mukai E, Toyoda Y, Miwa I, and Seino Y.** A novel glucokinase regulator in

- 44 -

pancreatic β cells: precursor of propionyl-CoA carboxylase β subunit interacts with glucokinase and augments its activity. *J Biol Chem* 276: 2325–2328, 2001.

39. **Sweet IR, Li G, Najafi H, Berner D, and Matschinsky FM.** Effect of a glucokinase inhibitor on energy production and insulin release in pancreatic islets. *Am J Physiol Endocrinol Metab* 271: E606–E625, 1996.

40. **Takahashi N, Kadowaki T, Yazaki Y, Ellis-Davies GC, Miyashita Y, and Kasai H.** Post-priming actions of ATP on Ca^{2+}-dependent exocytosis in pancreatic beta cells. *Proc Natl Acad Sci USA* 96: 760–765, 1999.

41. **Uchizono Y, Iwase M, Nakamura U, Sasaki N, Goto D, and Iida M.** Tacrolimus impairment of insulin secretion in isolated rat islets occurs at multiple distal sites in stimulus-secretion coupling. *Endocrinology* 145: 2264–2272, 2004.

42. **Velho G, Froguel P, Clement K, Pueyo ME, Rakotoambinina B, Zouali H, Passa P, Cohen D, and Robert JJ.** Primary pancreatic β-cell secretory defect caused by mutations in glucokinase gene in kindreds of maturity onset diabetes of the young. *Lancet* 340: 444–448, 1992.
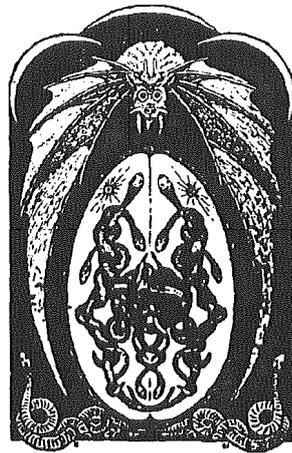
Chronic exposure to β-hydroxybutyrate inhibits glucose-induced insulin release from pancreatic islets by decreasing NADH contents

Mihoko Takehiro,[1] Shimpei Fujimoto,[1] Makiko Shimodahira,[1] Dai Shimono,[1] Eri Mukai,[1] Koichiro Nabe,[1]
Razvan Gheorghe Radu,[1] Rieko Kominato,[1] Yo Aramaki,[1] Yutaka Seino,[1,2] and Yuichiro Yamada[1]

[1]Department of Diabetes and Clinical Nutrition, Graduate School of Medicine,
Kyoto University, Kyoto; and [2]Kansai-Denryoku Hospital, Osaka, Japan

Submitted 5 April 2004; accepted in final form 9 October 2004

Takehiro, Mihoko, Shimpei Fujimoto, Makiko Shimodahira, Dai Shimono, Eri Mukai, Koichiro Nabe, Razvan Gheorghe Radu, Rieko Kominato, Yo Aramaki, Yutaka Seino, and Yuichiro Yamada. Chronic exposure to β-hydroxybutyrate inhibits glucose-induced insulin release from pancreatic islets by decreasing NADH contents. Am J Physiol Endocrinol Metab 288: E372–E380, 2005. First published October 12, 2004; doi:10.1152/ajpendo.00157.2004.—To investigate the effects of chronic exposure to ketone bodies on glucose-induced insulin secretion, we evaluated insulin release, intracellular Ca^{2+} and metabolism, and Ca^{2+} efficacy of the exocytotic system in rat pancreatic islets. Fifteen-hour exposure to 5 mM D-β-hydroxybutyrate (HB) reduced high glucose-induced insulin secretion and augmented basal insulin secretion. Augmentation of basal release was derived from promoting the Ca^{2+}-independent and ATP-independent component of insulin release, which was suppressed by the GDP analog. Chronic exposure to HB affected mostly the second phase of glucose-induced biphasic secretion. Dynamic experiments showed that insulin release and NAD(P)H fluorescence were lower, although the intracellular Ca^{2+} concentration ($[Ca^{2+}]_i$) was not affected 10 min after exposure to high glucose. Additionally, $[Ca^{2+}]_i$ efficacy in exocytotic system at clamped concentrations of ATP was not affected. NADH content, ATP content, and ATP-to-ADP ratio in the HB-cultured islets in the presence of high glucose were lower, whereas glucose utilization and oxidation were not affected. Mitochondrial ATP production shows that the respiratory chain downstream of complex II is not affected by chronic exposure to HB, and that the decrease in ATP production is due to decreased NADH content in the mitochondrial matrix. Chronic exposure to HB suppresses glucose-induced insulin secretion by lowering the ATP level, at least partly by inhibiting ATP production by reducing the supply of NADH to the respiratory chain. Glucose-induced insulin release in the presence of aminooxyacetate was not reduced, which implies that chronic exposure to HB affects the malate/aspartate shuttle and thus reduces NADH supply to mitochondria.

islet; reduced nicotinamide adenine dinucleotide; adenosine 5′-triphosphate

KETONE BODIES ARE PRODUCED IN THE LIVER and are used peripherally as an energy source when glucose is not readily available. Ketosis is seen in various physiological conditions such as fasting, prolonged exercise, and high-fat diet. Hyperketonemia is also caused by absolute or relative insulin deficiency in type 1 diabetic patients or type 2 diabetic patients, respectively (18).

The importance of insulin in control of ketone body production in the liver is well established (18). The function of these substrates in regulating insulin output from pancreatic β-cells

is less well understood. In short-term exposure of <60 min, ketone bodies such as D-β-hydroxybutyrate (HB) are oxidized by islet cells and enhance insulin secretion in the presence of stimulatory levels of glucose (4, 10, 15, 28, 29, 31). However, little is known of the effect of prolonged exposure to ketone bodies on pancreatic β-cells and insulin secretion. Zhou et al. (47) have reported that 48-h exposure to HB reduces high glucose-induced insulin secretion from human pancreatic islets without affecting pyruvate dehydrogenase (PDH) activity or PDH kinase activity, although the mechanism of the inhibitory effect is unclear.

The mechanism of glucose-stimulated insulin release from pancreatic β-cells is well documented. Glucose entry into the β-cells accelerates glycolysis and glucose oxidation to increase the ATP content and ATP-to-ADP ratio, which closes the ATP-sensitive K^+ (K_{ATP}) channels. The decrease in K^+ conductance depolarizes the membrane and opens the voltage-dependent Ca^{2+} channels (VDCC). Increased Ca^{2+} influx through VDCCs increases the intracellular Ca^{2+} concentration ($[Ca^{2+}]_i$) to a level that triggers exocytosis of the insulin granules (13). It has been shown that glucose can also promote insulin release K_{ATP} channel independently by increasing Ca^{2+} efficacy in stimulation-secretion coupling, which may be due at least in part to the direct effect of increased ATP derived from glucose metabolism on exocytosis (1, 13). The effect of chronic exposure to ketone bodies in this mechanism is not known, however.

In the present study, insulin release, intracellular Ca^{2+} and metabolism, and the efficacy of Ca^{2+} in the exocytotic system were investigated in HB-exposed islets.

MATERIALS AND METHODS

Materials. NADH, ADP, 2-amino-2-methyl-1-propanol, oxaloacetate, RPMI 1640 medium, alcohol dehydrogenase, aspartate transaminase, malate dehydrogenase, GDPβS, diadenosine pentaphosphate (DAPP), antimycin A, L-β-hydroxybutyrate, lithium acetoacetate, aminooxyacetate, and potassium aspartate were obtained from Sigma Chemicals (St. Louis, MO). Fura PE-3 AM was obtained from Calbiochem (La Jolla, CA). Succinate and HB were purchased from Aldrich (Steimheim, Germany). D-Hydroxybutyrate dehydrogenase was obtained from Toyobo (Osaka, Japan). ^3H_2O, [5-^3H]glucose, and [U-^{14}C]glucose were obtained from Amersham (Buckinghamshire, UK). All other reagents are of analytic grade and were obtained from Nacalai Tesque (Kyoto, Japan). Sodium acetoacetate was prepared and incubated for over 16 h at 20°C, from ethyl acetoacetate and NaOH (each 1 M), followed by three successive washes with diethyl

Address for reprint requests and other correspondence: S. Fujimoto, Dept. of Diabetes and Clinical Nutrition, Graduate School of Medicine, Kyoto Univ., 54 Shogoin Kawahara-cho, Sakyo-ku, Kyoto 606-8507, Japan (E-mail: fujimoto@metab.kuhp.kyoto-u.ac.jp).

ether to remove residual ethyl acetoacetate and ethanol formed by hydrolysis as previously described (29). The solution was then flushed with N_2 for 60 min and stored at $-80°C$.

Acetoacetate determination. Acetoacetate was determined as previously described (12). Briefly, the reaction mixture containing 50 µl of sample, 120 mM triethanolamine (pH 7.0), 375 µM NADH, 1 unit/ml D-hydroxybutyrate dehydrogenase, and 1.25 mg/ml oxamic acid in a total volume of 400 µl was incubated for 15 min at 37°C. The reaction was stopped by heating the mixture at 100°C for 2 min. The concentration was determined by measuring the decrease in absorbance at 340 nm using lithium acetoacetate as standard.

Animals. Male Wistar rats were obtained from Shimizu (Kyoto, Japan). The animals were fed standard lab chow ad libitum and allowed free access to water in an air-conditioned room with a 12:12-h light-dark cycle until used in the experiments. All experiments were carried out with rats aged 8-12 wk. The animals were maintained and used in accordance with the Guidelines for Animal Experiments of Kyoto University.

Islet isolation and culture. Islets of Langerhans were isolated from Wistar rats by collagenase digestion as described previously (6). Islets were cultured for 15 h in RPMI 1640 medium (containing 10% fetal calf serum, 100 IU/ml penicillin, 100 µg/ml streptomycin, and 8.3 mM glucose) with or without β-hydroxybutyrate and acetoacetate at 37°C in humidified air containing 5% CO_2.

Measurement of insulin release from intact islets. Insulin release from intact islets was monitored by use of static incubation and perifusion conditions, as described previously (6), with Krebs-Ringer bicarbonate buffer (KRBB) supplemented with 0.2% BSA and 10 mM HEPES adjusted to pH 7.4 (KRBB medium). For static incubation experiments, cultured islets were preincubated at 37°C for 30 min with 2.8 mM glucose. Groups of five islets were then batch incubated for 30 min in 0.7 ml of KRBB medium with 2.8 and 16.7 mM glucose. At the end of the incubation period, islets were pelleted by centrifugation (15,000 g, 180 s), and aliquots of the buffer were sampled.

For perifusion experiments, groups of 20 cultured islets were placed in each of the parallel chambers (400 µl each) of a perifusion apparatus and perifused with KRBB medium at a rate of 0.7 ml/min at 37°C. The medium was continuously gassed with 95% O_2-5% CO_2. Islets were perifused for 30 min to establish a stable insulin secretory rate at the basal level of glucose, and the glucose concentration was then raised to 16.7 mM.

The amount of immunoreactive insulin was determined by RIA, using rat insulin as standard (6). Insulin contents and DNA contents of islets were measured as previously described (8).

Measurement of $[Ca^{2+}]_i$ and reduced pyridine nucleotide fluorescence. For $[Ca^{2+}]_i$ measurement, cultured islets were loaded with fura PE-3 as previously described (7). The islets were immediately placed in a heat-controlled chamber on the stage of an inverted microscope kept at 36 ± 1°C, superfused with KRBB medium containing 2.8 mM glucose for 30 min, and subsequently exposed to the medium containing a high concentration of glucose. These islets were excited successively at 340 and 380 nm, and the fluorescence emitted at 510 nm was captured by a charge-coupled device (CCD) camera (Micro Max 5-MHz System; Roper Industries, Trenton, NJ). The 340-nm (F340) and 380-nm (F380) fluorescence signals were detected every 20 s, and the ratios (F340/F380) were calculated. In vitro calibration was performed as previously described (7). For reduced pyridine nucleotide [NAD(P)H] measurement, the islets without dye were excited successively at 360 nm, and the fluorescence emitted at 470 nm was captured every 20 s (9) by the CCD camera described above. Changes in NAD(P)H fluorescence signal were expressed as percent control values by dividing the signal at a given time by the average signal at 2.8 mM glucose during the last 1 min before stimulation.

Images of $[Ca^{2+}]_i$ and NAD(P)H were analyzed with the Meta Fluor image analyzing system (Universal Imaging, West Chester, PA).

Measurement of insulin release from permeabilized islets. Insulin release from permeabilized islets was determined as previously described (6). After preincubation with 2.8 mM glucose for 30 min, cultured islets were washed twice in cold potassium aspartate buffer (KA buffer) containing 140 mM potassium aspartate, 7 mM $MgSO_4$, 2.5 mM EGTA, 30 mM HEPES, and 0.5% BSA (pH 7.0), with $CaCl_2$ added to a Ca^{2+} concentration of 30 nM. The islets were permeabilized by high-voltage discharge in KA buffer and washed once with the same buffer. Groups of five electrically permeabilized islets were batch incubated for 30 min at 37°C in 0.4 ml of KA buffer with various concentrations of Ca^{2+} and ATP. At the end of the incubation period, permeabilized islets were pelleted by centrifugation (15,000 g, 180 s), and aliquots of the buffer were sampled for immunoreactive insulin determination.

Measurement of adenine nucleotide contents. After groups of cultured intact islets were preincubated at 2.8 mM glucose for 30 min, groups of 15 islets were batch incubated in 0.5 ml of KRBB medium containing 2.8 or 16.7 mM glucose at 37°C for 30 min. Incubation was stopped by the addition of 0.1 ml of 2 M $HClO_4$. The tubes were immediately mixed with vortex and sonicated in ice-cold water for 3 min. They were then centrifuged (3,000 g, 3 min), and a fraction (0.4 ml) of the supernatant was mixed with 100 µl of 2 M HEPES and 100 µl of 1 M Na_2CO_3. ATP and ADP were assayed by a luminometric method as previously described (8). For measurement of the sum of ATP + ADP, ADP was first converted into ATP by adding 210 µl of solution containing 20 mM HEPES (pH 7.75), 3 mM $MgCl_2$, 1.5 mM phospho*enol*pyruvate, and 2.2 U/ml pyruvate kinase to 70 µl of extracts, with incubation at 37°C for 30 min. The ATP concentration in solutions was measured by adding 200 µl of luciferin-luciferase solution (Turner Designs, Sunnyvale, CA) to a fraction of sample (100 µl) in a bioluminometer (Luminometer model 20e, Turner Designs). For measurement of ATP, the same procedure was performed except that the incubation step was done without pyruvate kinase. The ADP concentration was calculated as the difference between the value of ATP + ADP and ATP from the same sample. To draw a standard curve and to ascertain that the conversion of ADP into ATP was complete, blanks and ADP and ATP standards were run through the entire procedure, including the extraction steps.

Measurement of NADH contents. NADH contents were assayed with an enzymatic cycling system for NADH amplification (17, 45). After preincubation at 2.8 mM glucose, batches of 20 cultured islets were incubated in 50 µl of KRBB medium containing 2.8 or 16.7 mM glucose. After incubation at 37°C for 30 min, 20 µl of solution containing 40 mM NaOH and 0.5 mM cysteine were added to each tube. The tubes were immediately mixed with vortex and sonicated in the ice-cold water for 3 min. They were then centrifuged (3,000 g, 3 min), and a fraction (30 µl) of the supernatant was incubated for 20 min at 60°C to destroy any remaining NAD. For the first step in NADH amplification, the reaction mixture containing 30 µl of extract, 100 mM HEPES-NaOH buffer (pH 7.5), 1 mM dithiothreitol, 0.2 mg/ml BSA, 280 mM ethanol, 2 mM oxaloacetate, 16 U/ml alcohol dehydrogenase, and 4 U/ml malate dehydrogenase in a total volume of 100 µl was incubated for 30 min at 30°C. The reaction was stopped by heating the mixture at 100°C for 2 min. In the second step, malate formed in the first step was assayed by incubating 100 µl of sample solution in 50 mM 2-amino-2-methyl-1-propanol-HCl buffer (pH 9.9) containing 0.18 mM NAD, 0.1 mg/ml BSA, 9 mM glutamate, 0.8 unit/ml malate dehydrogenase, and 1 U/ml aspartate transaminase in a total volume of 600 µl for 30 min at 30°C. The NADH formed was measured by fluorometry (Shimazu RF-5000, Kyoto, Japan) at a 340-nm excitation and a 450-nm emission. To draw a standard curve, blanks and NADH standards were run through the entire procedure.

Measurement of mitochondrial ATP production. Mitochondrial suspension from cultured islets was prepared by repeated centrifugation, as previously described (14, 16, 19). First, isolated islets were homogenized in *solution A* consisting of (in mM) 50 HEPES, 100 KCl, 1.8 ATP, 1 EGTA, and 2 $MgCl_2$ and 0.5 mg/ml BSA (electrophoretically homogeneous; pH 7.00 at 37°C with KOH). After precipitation of cell debris and nuclei by centrifugation, the supernatant

was centrifuged more rapidly (10,000 g) to obtain a pellet containing the mitochondrial fraction. The precipitation diluted by 200 μl of *solution A* was centrifuged again and rinsed three times in solution consisting of (in mM) 20 HEPES, 3 KH_2PO_4, 1 EGTA, 12 sodium gluconate, 0.3 $MgCl_2$, 148 potassium gluconate, and 4 carnitine and 0.5 mg/ml BSA (electrophoretically homogeneous), adjusted to pH 7.10 with KOH (*solution B*). The mitochondrial fraction in 500 μl of *solution B* was kept on ice until use. To measure ATP production by oxidative phosphorylation, the reaction was started by adding 5 μl of mitochondrial suspension to 495 μl of prewarmed *solution B* (37°C) supplemented with the mitochondrial substrates, 50 μM ADP, and 1 μM DAPP adjusted to pH 7.10. DAPP is a specific inhibitor of adenylate kinase used to measure ATP production by oxidative phosphorylation exclusively. To normalize the mass of the intact mitochondria obtained, ATP production by adenylate kinase, one of the mitochondrial intermembrane kinases, was measured in the presence of ADP but without mitochondrial substrates or DAPP in parallel incubations (19–21). Reaction was stopped by addition of 0.5 μM antimycin A. The samples were cooled to room temperature, and ATP concentration in the solutions was measured by adding luciferin-luciferase solution to each sample with a bioluminometer. ATP production was determined as the ratio of ATP production by oxidative phosphorylation to that by adenylate kinase. To draw a standard curve, blank and ATP standards were added to parallel samples containing the complete incubation mixture except the mitochondrial suspension.

Measurement of glucose utilization and oxidation. Glucose utilization and oxidation were measured, using the previously described method (3) with a slight modification. Cultured islets were preincubated in KRBB medium with 2.8 mM glucose at 37°C for 30 min. For utilization, batches of 30 islets for each condition were incubated at 37°C for 90 min in 150 μl of medium containing 1.5 μCi of [5-^{3}H]glucose. Aliquots of the incubation medium (100 μl) and 20 μl of 1 M HCl were transferred to small tubes and placed into a glass vial containing 0.5 ml of H_2O. The capped vials were incubated overnight at 34°C to vaporize ^3H_2O from the solution. The inner tube was then lifted out, and the disintegrations per minute of water-melting ^3H_2O in the vial were counted. In a parallel incubation, the recovery ratio of ^3H_2O was measured with ^3H_2O. After subtraction of blank disintegrations per minute from sample disintegrations per minute, glucose utilization was calculated with the disintegrations per minute, specific radioactivity of [5-^{3}H]glucose, and recovery ratio of ^3H_2O. For oxidation, all procedures were the same as for utilization except the use of [U-^{14}C]glucose (0.5 μCi/tube) and 0.5 ml of hydroxide of hyamine 10-X (Packard, Meriden, CT) in place of [5-^{3}H]glucose and 0.5 ml of H_2O, respectively. After subtraction of blank disintegrations per minute from sample disintegrations per minute, glucose oxidation was calculated using the disintegrations per minute and specific radioactivity of [U-^{14}C]glucose.

Statistical analysis. Results are expressed as means ± SE. Statistical significance was evaluated by unpaired Student's t-test. $P < 0.05$ was considered significant.

RESULTS

Effect of chronic exposure to β-hydroxybutyrate on glucose-induced insulin release from intact islets. Addition of 10 mM HB to RPMI 1640 medium did not alter the H^+ concentration measured by the H^+ electrode (data not shown). Exposure to 1 mM HB for 15 h did not alter 16.7 mM glucose-induced and basal insulin release. However, exposure to 2 mM HB reduced 16.7 mM glucose-induced insulin release but enhanced basal insulin release. No further inhibitory effect on high glucose-induced insulin release and no further enhancement of basal insulin release at 5 mM HB were observed (Table 1, *top*). Insulin release in the presence of 200 μM diazoxide, 16.7 mM

glucose, and 30 mM K^+ from HB-cultured islets was also reduced by chronic exposure to 5 mM HB for 15 h (HB 1.22 ± 0.03 vs. control 2.15 ± 0.09 ng·islet^{-1}·30 min^{-1}, $n = 5$, $P < 0.01$). Exposure to 5 mM L-β-hydroxybutyrate for 15 h did not alter 16.7 mM glucose-induced and basal insulin release (Table 1, *bottom*). The DNA contents and insulin contents of islets cultured with 5 mM HB for 15 h were similar to controls (DNA contents: HB 26.6 ± 1.9 vs. control 27.1 ± 1.8 ng/islet, $n = 30$, not significant; insulin contents: HB 34.3 ± 1.9 vs. control 30.6 ± 1.4 ng/islet, $n = 30$, not significant).

In perifusion experiments, insulin release from HB-cultured islets in the presence of 2.8 mM glucose for 5 min before high-glucose exposure was increased compared with control islets (Fig. 1A, *inset*; mean value from −5 to 0 min: HB 0.21 ± 0.01 vs. control 0.16 ± 0.01 ng·20 islets^{-1}·min^{-1}, $n = 6$, $P < 0.01$). Insulin release began to elevate ∼1 min after exposure to high glucose in both groups of islets (Fig. 1A). Insulin release from HB-cultured islets 1–10 min after 16.7 mM glucose exposure was similar to that from control islets. Insulin release from HB-cultured islets for the second and third 10-min period after high-glucose exposure was less than from control islets (Fig. 1B; mean value from 20 to 30 min: HB 1.93 ± 0.14 vs. control 2.66 ± 0.07 ng·20 islets^{-1}·min^{-1}, $n = 6$, $P < 0.01$).

Effect of chronic exposure to acetoacetate on glucose-induced insulin release from intact islets. Because acetoacetate (AcA) is spontaneously decarboxylated to acetone, a decline in the concentration of AcA in the medium may occur during the culture period. As expected, decreases in the concentrations of AcA were observed in the medium; however, >65% AcA remained in the medium at the end of the 15-h culture period (Table 2). Exposure to AcA (initial concentration 2–10 mM) for 15 h did not affect 16.7 mM glucose-induced insulin release. However, chronic exposure to high concentrations of AcA (initial concentration 10 mM) augmented basal insulin release (Table 2).

Table 1. *Effect of chronic exposure to D-β-hydroxybutyrate on glucose-induced insulin release from intact islets*

Experimental Condition During Culture	Insulin Release, ng·islet^{-1}·30 min^{-1}	
	Basal (2.8 mM glucose)	Stimulated (16.7 mM glucose)
Control	0.21±0.01	2.89±0.14
1 mM D-HB	0.24±0.01	2.63±0.15
2 mM D-HB	0.29±0.01*	2.46±0.13†
5 mM D-HB	0.31±0.02*	2.18±0.13*
7 mM D-HB	0.29±0.02*	2.24±0.12*
10 mM D-HB	0.26±0.01*	2.15±0.12*
Control	0.19±0.01	2.81±0.11
5 mM L-HB	0.21±0.02	2.99±0.13
5 mM D-HB	0.32±0.03*	2.26±0.15*

Values are means ± SE of 12 (*top*) and 16 (*bottom*) determinations from several experiments. Intact islets were cultured under the conditions indicated for 15 h. After cultured islets were preincubated with 2.8 mM glucose for 30 min, insulin release in the presence of 2.8 and 16.7 mM glucose for 30 min was determined. *Top:* concentration-dependent effect of D-β-hydroxybutyrate (D-HB) on insulin release. *Bottom:* effect of chronic exposure to D-HB and L-β-hydroxybutyrate (L-HB) on insulin release. *$P < 0.01$ vs. corresponding control (cultured without HB). †$P < 0.05$ vs. corresponding control (cultured without HB).
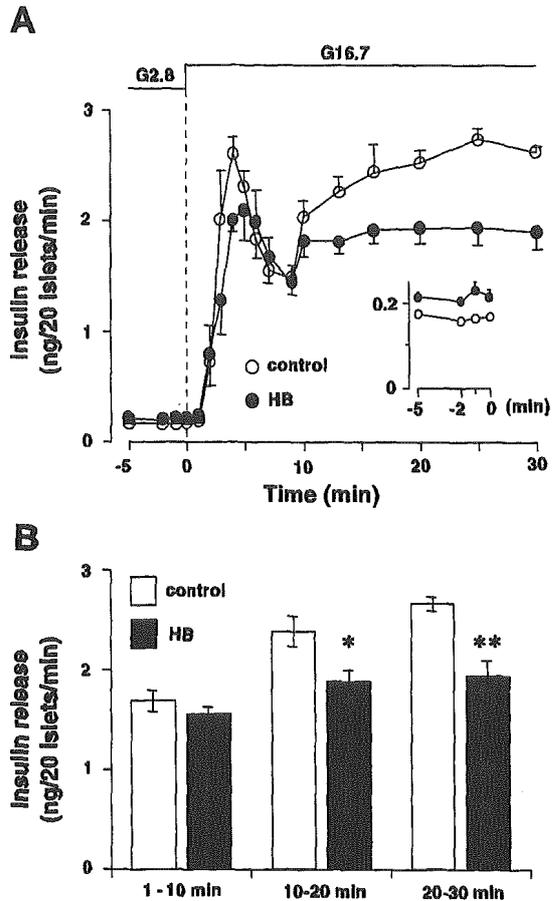
A

B

Fig. 1. Effect of D-β-hydroxybutyrate (HB) on biphasic 16.7 mM glucose-induced insulin release from intact islets. Islets were cultured with or without 5 mM HB for 15 h. After 2 groups of islets were perifused for 30 min (−30 to 0 min) with 2.8 mM glucose (G2.8), they were stimulated with 16.7 mM glucose (G16.7; 0–30 min). Values represent means ± SE of 6 determinations in the same experiments. Experiments using the same protocol were repeated 3 times to ascertain reproducibility. *A*: time course of high glucose-induced biphasic insulin release from control and HB-cultured islets. All values in HB-treated islets after 13 min, except those at 16 min, were significantly less than the corresponding control values (at 13 min, $P < 0.05$; at 20, 25, and 30 min, $P < 0.01$). *Inset*: time course of basal insulin release for 5 min (−5 to 0 min) in the same experiment. All values in HB-treated islets from −5 to 0 min were significantly greater than the corresponding control values (at −5 and 0 min, $P < 0.05$; at −2 and 0 min, $P < 0.01$). *B*: average values of insulin release from control and HB-cultured islets during the time indicated. Values are calculated from the data in *A*. *$P < 0.05$ vs. control; **$P < 0.01$ vs. control.

[Ca²⁺]ᵢ elevation in intact islets induced by a high concentration of glucose. Figure 2*A* shows $[Ca^{2+}]_i$ elevation induced by a high concentration of glucose in control and HB-cultured islets. In the presence of 2.8 mM glucose for 5 min before exposure to high glucose, $[Ca^{2+}]_i$ of HB-cultured islets was higher than in control islets (average from −5 to 0 min: HB 134.8 ± 10.4, $n = 17$, vs. control 86.7 ± 7.6 nM, $n = 13$, $P < 0.01$). However, $[Ca^{2+}]_i$ of HB-cultured islets at 1–10 min and for the second and third 10-min period after exposure to high glucose was similar to that of controls (Fig. 2*B*).

Insulin release from electrically permeabilized islets. In the presence of 5 mM ATP, raising the Ca^{2+} concentration from 30 nM to 3 μM elicited a concentration-dependent increase in insulin release from both electrically permeabilized control and

HB-cultured islets. In the presence of 5 mM ATP, insulin release at 30 nM, 100 nM, 1 μM, and 3 μM Ca^{2+} was greater in HB-cultured islets than in control islets (Fig. 3*A*). Augmentation of insulin release at 30 nM Ca^{2+} in HB-cultured islets also was found in the absence of ATP, indicating an effect of the ATP-independent and Ca^{2+}-independent component of insulin release (6) (Fig. 3*B*). When the increment of insulin release in the presence of 30 nM Ca^{2+}, which is due to chronic exposure to HB, was subtracted from the insulin release from HB-cultured islets to evaluate Ca^{2+}-dependent components of insulin release (7), the values at 100 nM, 1 μM, and 3 μM were found to be similar to the values from control islets (Fig. 3*A*). Insulin release without ATP at 30 nM Ca^{2+} from control islets was not affected by 500 μM GDPβS, a stable GDP analog, although that from HB-cultured islets was significantly suppressed by the analog (Fig. 3*B*).

Time course of NAD(P)H fluorescence in intact islets. NAD(P)H fluorescence began to elevate immediately after exposure to high glucose in both groups of islets and reached plateau within 5 min after exposure (Fig. 4). Attenuation of NAD(P)H fluorescence was observed from 2 min in HB-cultured islets (at 2 min: HB 1.16 ± 0.01, $n = 15$, vs. control 1.38 ± 0.03 arbitrary units, $n = 12$, $P < 0.01$). The average of fluorescence during the first, second, and third 10-min period was lower in HB-cultured islets than in control islets (from 0 to 10 min: HB 1.23 ± 0.01, $n = 15$, vs. control 1.50 ± 0.03, $n = 12$, $P < 0.01$; from 10 to 20 min: HB 1.32 ± 0.02, $n = 15$, vs. control 1.68 ± 0.04, $n = 12$, $P < 0.01$; from 20 to 30 min: HB 1.31 ± 0.03, $n = 15$, vs. control 1.68 ± 0.04 arbitrary units, $n = 12$, $P < 0.01$).

Reduced pyridine nucleotide contents and adenine nucleotide contents. NADH contents in the presence of 16.7 mM were greater than in the presence of 2.8 mM glucose in both control and HB-cultured islets. NADH contents of HB-cultured islets in the presence of 2.8 mM glucose and in the presence of 16.7 mM glucose were more and less than control islets, respectively (Table 3, *top*). The ATP contents and the ATP-to-ADP ratio in the presence of 16.7 mM were greater than in the presence of 2.8 mM glucose in both control and HB-cultured islets. The ATP contents and ATP-to-ADP ratio of HB-cul-

Table 2. *Effect of chronic exposure to acetoacetate on glucose-induced insulin release from intact islets*

Experimental Condition During Culture, mM		Insulin Release, ng·islet⁻¹·30 min⁻¹	
Initial	After 15 h	Basal (2.8 mM glucose)	Stimulated (16.7 mM glucose)
Control		0.21 ±0.02	2.81±0.12
2.0	1.3	0.21 ±0.02	2.79±0.09
5.0	4.0	0.18 ±0.01	2.82±0.15
10.0	9.1	0.31 ±0.02*	3.06±0.20

Values are means ± SE of 15 determinations from 3 experiments. Effect of chronic exposure to various concentrations of acetoacetate on insulin release. Intact islets were cultured under the conditions indicated for 15 h. Initial concentration of acetoacetate in the medium is indicated. At the end of the culture period, acetoacetate concentrations in the medium were determined. After cultured islets were preincubated with 2.8 mM glucose for 30 min, insulin release in the presence of 2.8 and 16.7 mM glucose for 30 min was determined. *$P < 0.01$ vs. corresponding control (cultured without acetoacetate).
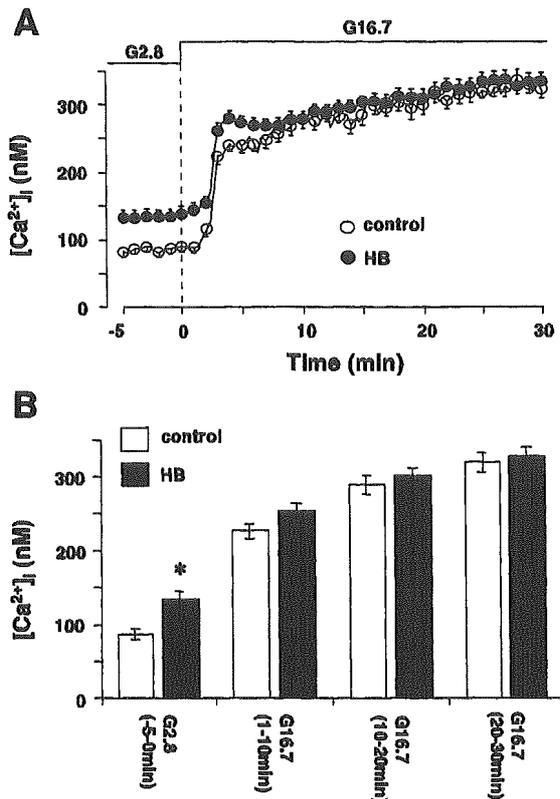
Fig. 2. Intracellular Ca^{2+} concentration ($[Ca^{2+}]_i$) elevation induced by 16.7 mM glucose in control and HB-cultured intact islets. Islets were cultured with or without 5 mM HB for 15 h. After preincubation with 2.8 mM glucose for 30 min, the islets were stimulated with 16.7 mM glucose at time 0. A: time course of $[Ca^{2+}]_i$ in control and HB-cultured islets. Values represent means ± SE of 13 (control) or 17 (HB) determinations from several experiments. B: average values of $[Ca^{2+}]_i$ from control and HB-cultured islets during the time indicated. Values are calculated from the data in A. *$P < 0.01$ vs. control.

tured islets in the presence of 16.7 mM glucose were less than in control islets (Table 3, *bottom*).

ATP production by mitochondria from islets. ATP production by mitochondria from control and HB-cultured islets in the presence of various substrates and inhibitors is shown in Table 4. ATP production by mitochondria from HB-cultured islets in the presence of succinate was decreased compared with that from control islets. Antimycin A, a complex III inhibitor in the respiratory chain, inhibited ATP production dramatically in the presence of succinate in both control and HB-cultured islets. Rotenone, a complex I inhibitor in the respiratory chain, also inhibited ATP production in the presence of succinate in both control and HB-cultured islets. However, in the presence of succinate and rotenone, no significant difference in ATP production was observed in control and HB-cultured islets. Mitochondrial ATP production of HB-cultured islets was similar to that of control islets in the presence of tetramethyl-*p*-phenyldiamine and ascorbate.

Glucose utilization and glucose oxidation. Glucose utilization and glucose oxidation in the presence of 16.7 mM glucose were greater than in the presence of 2.8 mM glucose in both control and HB-cultured islets. Glucose utilization and glucose oxidation of HB-cultured islets in the presence of 2.8 mM glucose were greater than in control islets. However, glucose

utilization and glucose oxidation of HB-cultured islets in the presence of 16.7 mM glucose were not different from those of control islets (Table 5).

Insulin release in the presence of aminooxyacetate. Glucose (16.7 mM)-induced insulin release from HB-cultured islets was reduced compared with that from control islets (HB 2.22 ± 0.08 vs. control 2.89 ± 0.16 ng·islet^{-1}·30 min^{-1}, $n = 7$, $P < 0.01$). Aminooxyacetate (AOA), an aspartate aminotransferase inhibitor, reduced 16.7 mM glucose-induced insulin release from both control and HB-cultured islets. However, in the presence of AOA, 16.7 mM glucose-induced insulin release from HB-cultured islets was not different from that of control
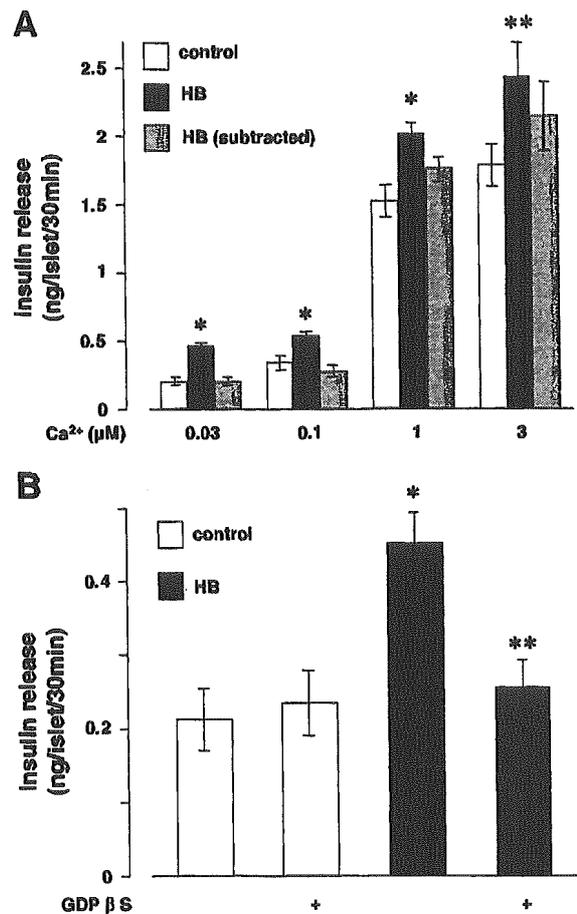

Fig. 3. Effect of HB on insulin release from electrically permeabilized islets in the presence of various concentrations of Ca^{2+} with or without 5 mM ATP. Islets were cultured with or without 5 mM HB for 15 h. After preincubation with 2.8 mM glucose for 30 min, islets were electrically permeabilized and incubated in the indicated medium. A: insulin release from control and HB-cultured islets in the presence of 5 mM ATP. Values obtained by subtracting the increment in insulin release in the presence of 30 nM Ca^{2+} with 5 mM ATP due to chronic exposure to HB from the value of insulin release from HB-cultured islets are indicated. Values represent means ± SE of 15 (control) and 16 (HB) determinations from several experiments. *$P < 0.01$ vs. corresponding control; **$P < 0.05$ vs. corresponding control. B: insulin release from control and HB-cultured islets in the presence of 30 nM Ca^{2+} and in the absence of ATP with (+) or without 500 μM GDPβS. GDPβS was present during incubation of permeabilized islets with 30 nM Ca^{2+} and without ATP (for 30 min). Values represent means ± SE of 8 determinations from 2 experiments. *$P < 0.01$ vs. corresponding control without GDPβS; **$P < 0.01$ vs. HB-cultured islets without GDPβS.
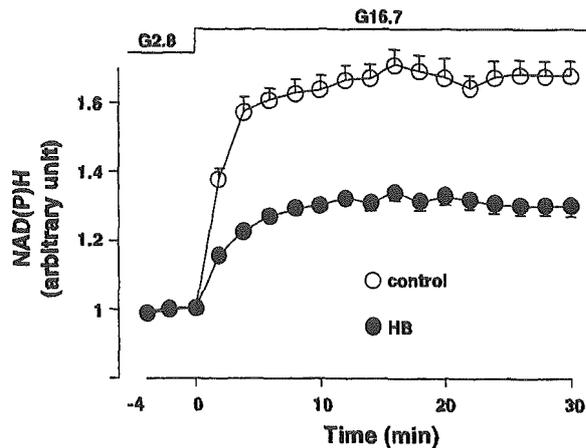
Fig. 4. Time course of NAD(P)H elevation induced by 16.7 mM glucose in control and HB-cultured islets. Islets were cultured with or without 5 mM HB for 15 h. After perifusion with 2.8 mM glucose for 30 min, they were exposed to 16.7 mM glucose at *time 0* for 30 min. NAD(P)H signals were measured at 20-s intervals from −4 to 30 min. Values represent means ± SE of 12 (control) and 15 (HB) determinations from several experiments.

islets (HB 1.98 ± 0.06 vs. control 1.91 ± 0.07 ng·islet^{-1}·30 min^{-1}, $n = 7$, not significant; Fig. 5).

DISCUSSION

We find that chronic exposure to HB reduces high glucose-induced insulin secretion and augments basal insulin secretion from pancreatic islets. Insulin secretion is reduced by diminished ATP, which is at least partly due to lower ATP production resulting from the reduced supply of NADH to the respiratory chain. Basal insulin secretion is increased due to augmentation of the Ca^{2+}-independent and ATP-independent component of insulin release, in which a GTP-sensitive site may play a role.

In the present study, chronic exposure to >2 mM HB affected insulin secretion, this concentration of HB augmenting glucose-induced insulin acutely in vitro (4, 10, 15, 28, 29, 31) and being frequently observed in serum in various pathophysiological states (18). Acute exposure to the L-isomer was ineffective on insulin release, presumably due to no capacity to

Table 3. *Reduced pyridine nucleotide and adenine nucleotides contents in the presence of basal and stimulated levels of glucose in control and HB-cultured islets*

	Control Islets		HB-Cultured Islets	
	2.8 mM	16.7 mM	2.8 mM	16.7 mM
NADH, fmol/islet	89±7	375±35*	138±11†	256±8*†
ATP, pmol/islet	6.53±0.36	8.26±0.36*	5.91±0.23	6.78±0.35†‡
ADP, pmol/islet	2.21±0.16	1.51±0.08*	1.93±0.09	1.56±0.14‡
ATP-to-ADP ratio	3.06±0.14	5.56±0.17*	3.12±0.10	4.71±0.35*§

Values are means ± SE of 11 (*top*) and 17 (*bottom*) determinations from several experiments. Islets were cultured with or without 5 mM HB for 15 h. After cultured intact islets were preincubated with 2.8 mM glucose for 30 min, they were incubated with 2.8 and 16.7 mM glucose for 30 min. Reaction was stopped, and nucleotides contents were determined. *$P < 0.01$ vs. corresponding islet incubated with 2.8 mM glucose. †$P < 0.01$ vs. corresponding control cultured without HB. ‡$P < 0.05$ vs. corresponding islet incubated with 2.8 mM glucose. §$P < 0.05$ vs. corresponding control cultured without HB.

Table 4. *ATP production by mitochondria from control and HB-cultured islets*

	Mitochondrial ATP Production	
Experimental Conditions	Control islets	HB-cultured islets
1 mM Succinate	2.99±0.20	2.42±0.10*
1 mM Succinate + 1 μM rotenone	2.18±0.16†	1.98±0.12†
20 mg/ml TMPD + 2 mM ascorbate	1.04±0.09	0.98±0.09
1 mM Succinate + 0.5 μM antimycin A	0.09±0.02‡	0.06±0.02‡

Values are means ± SE of 5 determinations from 5 experiments. Islets were cultured with or without 5 mM HB for 15 h. Mitochondrial suspension was obtained from control and HB-cultured islets. Mitochondrial ATP production is indicated as the ratio to ATP production from adenylate kinase, which was determined from the same sample in parallel incubation. TMPD, tetramethyl-*p*-phenyldiamine. *$P < 0.05$ vs. corresponding control cultured without HB. †$P < 0.05$ vs. corresponding succinate alone. ‡$P < 0.01$ vs. corresponding succinate alone.

oxidize the isomer in islets (4, 28). To exclude nonspecific effects of HB, the chronic effect of the L-isomer was also examined. Because the L-isomer did not affect insulin release, the effect of the D-isomer is presumably linked to its metabolism. Moreover, chronic exposure to AcA, another ketone body, did not affect glucose-induced insulin release. HB is oxidized to AcA by D-β-hydroxybutyrate dehydrogenase, a mitochondrial enzyme, also present in islets (28), producing NADH in mitochondria. Accordingly, alteration of mitochondrial redox potential during culture may be involved in reduced glucose-induced insulin release from HB-cultured islets. Interestingly, acute exposure to exogenous HB or AcA increases or decreases [6-^{14}C]glucose oxidation (28), respectively, which is strongly affected by anaplerosis (41). Anaplerosis plays an important role in determination of the cytosolic level of metabolic factors, including malonyl-CoA (5), NADPH (24), and nonessential amino acids (41) in pancreatic β-cells. The chronic effects of these factors should be taken into account when considering reduced glucose-induced insulin release by HB.

In pancreatic β-cells, intracellular Ca^{2+} and ATP are the most important regulators of insulin secretion, although there may be other independent metabolic signals (2, 25–27, 34). Ca^{2+} and ATP directly affect the exocytotic system and enhance insulin release synergistically in experiments using single β-cells (37, 43) and permeabilized islets (7). In the present study, we have compared [Ca^{2+}]$_i$, intracellular ATP, and

Table 5. *Glucose oxidation and glucose utilization in control and HB-cultured islets*

	2.8 mM Glucose	16.7 mM Glucose
Glucose utilization		
Control islets	25.1±2.0	84.6±6.7*
HB-cultured islets	39.5±3.9†	90.1±5.1*
Glucose oxidation		
Control islets	3.1±0.4	18.4±3.7*
HB-cultured islets	7.1±0.8†	20.8±1.9*

Values are mean glucose metabolism ± SE (in pmol·islet^{-1}·90 min^{-1}) of 7 (glucose utilization) and 9 (glucose oxidation) determinations from several experiments. Islets were cultured with or without 5 mM HB for 15 h. After cultured intact islets were preincubated with 2.8 mM glucose for 30 min, they were incubated with 2.8 and 16.7 mM glucose for 90 min. *$P < 0.01$ vs. corresponding control incubated with 2.8 mM glucose. †$P < 0.01$ vs. corresponding control cultured without HB.
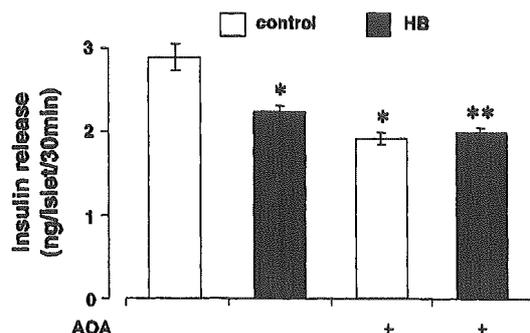
Fig. 5. Glucose (16.7 mM)-induced insulin release from control and HB-cultured islets in the presence of aminooxyacetate (AOA). Islets were cultured with or without 5 mM HB for 15 h. After cultured intact islets were preincubated with 2.8 mM glucose for 30 min, they were incubated with 16.7 mM glucose with (+) or without 5 mM AOA for 30 min. Values represent means ± SE of 7 determinations. $*P < 0.01$ vs. control without AOA; $**P < 0.05$ vs. HB-cultured islets without AOA.

$[Ca^{2+}]_i$ efficacy in the exocytotic system at clamped concentrations of ATP in control and HB-exposed islets.

Chronic exposure to HB decreases insulin release by 16.7 mM glucose during a short period around the peak in the first phase and mostly during the second phase of biphasic secretion, 10 min after exposure. $[Ca^{2+}]_i$ in the presence of 16.7 mM glucose in HB-cultured islets was similar to that in control islets during the second phase. Moreover, insulin release in the presence of diazoxide, high glucose, and a depolarizing concentration of K^+, in which $[Ca^{2+}]_i$ is clamped independently of glucose metabolism (10), is also reduced by chronic exposure to HB. Apparently, $[Ca^{2+}]_i$ does not play a role in the lower response to high glucose in HB-cultured islets. In addition, Ca^{2+} efficacy at clamped concentration of ATP in the exocytotic system was similar in the two groups of islets. On the other hand, NAD(P)H fluorescence was less in the HB-cultured islets in the presence of high glucose. Moreover, both ATP contents and ATP-to-ADP ratio of HB-cultured islets 30 min after exposure to high glucose were reduced compared with control islets. Decreased intracellular ATP reduces Ca^{2+} efficacy in the exocytotic system (7, 37, 43). Therefore, the lower ATP level due to the reduced redox state may play a major role in the attenuation of insulin secretion from HB-cultured islets in response to high glucose.

NAD(P)H autofluorescence dominantly reflects the redox state of mitochondria (32) and is widely used as an index of the intracellular redox state in intact islets (9, 33, 36). However, the method cannot discriminate between NADH and NADPH signals. Therefore, NADH, the supply of which accelerates mitochondrial oxidative phosphorylation, was determined using the enzymatic method. NADH contents of HB-cultured islets were lower in the presence of high glucose, partly accounting for the decreased ATP level in these islets.

To determine whether oxidative phosphorylation in the mitochondrial respiratory chain is suppressed in HB-cultured islets, mitochondrial ATP production was examined in the presence of various substrates and inhibitors. In the presence of succinate, which directly renders electrons to complex II (39), ATP production in HB-cultured islets is less than in controls. The fact that ATP production in both groups of islets in the presence of succinate is partially inhibited by rotenone, a

complex I inhibitor (39), indicates that increased NADH derived from succinate also renders electrons to complex I and that electrons from complex I, in addition to electrons from complex II, augment oxidative phosphorylation in the presence of succinate. Tetramethyl-p-phenyldiamine with ascorbate renders electrons to cytochrome C, which transfers electrons to complex IV (39). The fact that ATP production in the presence of succinate and rotenone and in the presence of tetramethyl-p-phenyldiamine and ascorbate is similar in the two groups of islets indicates that the respiratory chain downstream of complex II is not affected by chronic exposure to HB. Accordingly, the decrease in ATP production in the presence of succinate may be due to decreased NADH content in the matrix of mitochondria derived from succinate.

NADH in the matrix of mitochondria is produced in a reaction catalyzed by isocitrate dehydrogenase, α-ketoglutarate dehydrogenase, and malate dehydrogenase in the TCA cycle, and by PDH (23, 38). Malate dehydrogenase also participates in the malate/aspartate shuttle, which carries NADH produced in cytosol to the matrix of mitochondria (22, 40). PDH activity is not affected by chronic exposure to HB in human islets (47). The fact that glucose utilization and glucose oxidation were not affected indicates that isocitrate dehydrogenase, α-ketoglutarate dehydrogenase, and PDH, which catalyze reactions accompanying production of NADH and CO_2, were not affected by chronic exposure to HB. Malate dehydrogenase catalyzes reactions that produce NADH without production of CO_2 that are involved in both the TCA cycle and malate/aspartate shuttle. AOA (5 mM) reduced glucose-induced insulin release from rat islets without affecting glucose oxidation, because AOA does not affect the TCA cycle and inhibits the malate/aspartate shuttle by blocking transamination reactions (30). Glucose-induced insulin release in the presence of AOA was not reduced by chronic exposure to HB, suggesting that chronic exposure to HB affects the malate/aspartate shuttle.

With the use of electrically permeabilized islets incubated at low Ca^{2+} without ATP, it was revealed that augmentation of basal insulin release from HB-cultured islets does not necessarily require elevation of $[Ca^{2+}]_i$, although $[Ca^{2+}]_i$ was higher in HB-cultured islets in the presence of basal levels of glucose than in control islets. This augmentation is not due to nonspecific leakage of insulin and to slow washout of insulin, since it was suppressed by the GDP analog, which is also compatible with the fact that GTP augments insulin release in the exocytotic process directly and Ca^{2+} independently (35).

Postprandial insulin release is inhibited in vivo in the starved state (11, 42, 46) and in type 2 diabetic patients with ketosis (44). Although the present results suggest suppressed insulin release in such pathophysiological conditions, these results may well not be found in vivo, as elevation of basal insulin secretion is not observed in the fasting state.

REFERENCES

1. **Aizawa T, Komatsu M, Asanuma N, Sato Y, and Sharp GWG.** Glucose action "beyond ionic events" in the pancreatic β cell. *Trends Pharmacol Sci* 19: 496–499, 1998.
2. **Antinozzi PA, Segall L, Prentki M, McGarry JD, and Newgard CB.** Molecular or pharmacologic perturbation of the link between glucose and lipid metabolism is without effect on glucose-stimulated insulin secretion. A re-evaluation of the long-chain acyl-CoA hypothesis. *J Biol Chem* 273: 16146–16154, 1998.
3. **Ashcroft SJ, Weerasinghe LC, Bassett JM, and Randle PJ.** The pentose cycle and insulin release in mouse pancreatic islets. *Biochem J* 126: 525–532, 1972.
4. **Biden TJ and Taylor KW.** Effects of ketone bodies on insulin release and islet-cell metabolism in the rat. *Biochem J* 212: 371–377, 1983.
5. **Farfari S, Schulz V, Corkey B, and Prentki M.** Glucose-regulated anaplerosis and cataplerosis in pancreatic β-cells: possible implication of a pyruvate/citrate shuttle in insulin secretion. *Diabetes* 49: 718–726, 2000.
6. **Fujimoto S, Ishida H, Kato S, Okamoto Y, Tsuji K, Mizuno N, Ueda S, Mukai E, and Seino Y.** The novel insulinotropic mechanism of pimobendan: direct enhancement of the exocytotic process of insulin secretory granules by increased Ca^{2+} sensitivity in β-cells. *Endocrinology* 139: 1133–1140, 1998.
7. **Fujimoto S, Mukai E, Hamamoto Y, Takeda T, Takehiro M, Yamada Y, and Seino Y.** Prior exposure to high glucose augments depolarization-induced insulin release by mitigating the decline of ATP level in rat islets. *Endocrinology* 143: 213–221, 2002.
8. **Fujimoto S, Tsuura Y, Ishida H, Tsuji K, Mukai E, Kajikawa M, Hamamoto Y, Takeda T, Yamada Y, and Seino Y.** Augmentation of basal insulin release from rat islets by preexposure to a high concentration of glucose. *Am J Physiol Endocrinol Metab* 279: E927–E940, 2000.
9. **Gilon P and Henquin JC.** Influence of membrane potential changes on cytoplasmic Ca^{2+} concentration in an electrically excitable cell, the insulin-secreting pancreatic B-cell. *J Biol Chem* 267: 20713–20720, 1992.
10. **Goberna R, Tamarit J Jr, Osorio J, Fussganger R, Tamarit J, and Pfeiffer EF.** Action of B-hydroxy butyrate, acetoacetate and palmitate on the insulin release in the perfused isolated rat pancreas. *Horm Metab Res* 6: 256–260, 1974.
11. **Grey NJ, Goldring S, and Kipnis DM.** The effect of fasting, diet, and actinomycin D on insulin secretion in the rat. *J Clin Invest* 49: 881–889, 1970.
12. **Harano Y, Ohtsuki M, Ida M, Kojima H, Harada M, Okanishi T, Kashiwagi A, Ochi Y, Uno S, and Shigeta Y.** Direct automated assay method for serum or urine levels of ketone bodies. *Clin Chim Acta* 151: 177–183, 1985.
13. **Henquin JC.** Triggering and amplifying pathways of regulation of insulin secretion by glucose. *Diabetes* 49: 1751–1760, 2000.
14. **Idahl LA and Lembert N.** Glycerol 3-phosphate-induced ATP production in intact mitochondria from pancreatic B-cells. *Biochem J* 312: 287–292, 1995.
15. **Ikeda T, Yoshida T, Ito Y, Murakami I, Mokuda O, Tominaga M, and Mashiba H.** Effect of β-hydroxybutyrate and acetoacetate on insulin and glucagon secretion from perfused rat pancreas. *Arch Biochem Biophys* 257: 140–143, 1987.
16. **Kajikawa M, Fujimoto S, Tsuura Y, Mukai E, Takeda T, Hamamoto Y, Takehiro M, Fujita J, Yamada Y, and Seino Y.** Ouabain suppresses glucose-induced mitochondrial ATP production and insulin release by generating reactive oxygen species in pancreatic islets. *Diabetes* 51: 2522–2529, 2002.
17. **Kato T, Berger SJ, Carter JA, and Lowry OH.** An enzymatic cycling method for nicotinamide-adenine dinucleotide with malic and alcohol dehydrogenases. *Anal Biochem* 53: 86–97, 1973.
18. **Laffel L.** Ketone bodies: a review of physiology, pathophysiology and application of monitoring to diabetes. *Diabetes Metab Res Rev* 15: 412–426, 1999.
19. **Lembert N and Idahl LA.** α-Ketoisocaproate is not a true substrate for ATP production by pancreatic β-cell mitochondria. *Diabetes* 47: 339–344, 1998.
20. **Lembert N, Idahl LA, and Ammon HP.** K-ATP channel independent effects of pinacidil on ATP production in isolated cardiomyocyte or pancreatic β-cell mitochondria. *Biochem Pharmacol* 65: 1835–1841, 2003.
21. **Lembert N, Joos HC, Idahl LA, Ammon HP, and Wahl MA.** Methyl pyruvate initiates membrane depolarization and insulin release by metabolic factors other than ATP. *Biochem J* 354: 345–350, 2001.
22. **MacDonald MJ.** Evidence for the malate aspartate shuttle in pancreatic islets. *Arch Biochem Biophys* 213: 643–649, 1982.
23. **MacDonald MJ.** Differences between mouse and rat pancreatic islets: succinate responsiveness, malic enzyme, and anaplerosis. *Am J Physiol Endocrinol Metab* 283: E302–E310, 2002.
24. **MacDonald MJ.** The export of metabolites from mitochondria and anaplerosis in insulin secretion. *Biochim Biophys Acta* 1619: 77–88, 2003.
25. **MacDonald MJ and Fahien LA.** Glutamate is not a messenger in insulin secretion. *J Biol Chem* 275: 34025–34027, 2000.
26. **Maechler P, Kennedy ED, Pozzan T, and Wollheim CB.** Mitochondrial activation directly triggers the exocytosis of insulin in permeabilized pancreatic β-cells. *EMBO J* 16: 3833–3841, 1997.
27. **Maechler P and Wollheim CB.** Mitochondrial glutamate acts as a messenger in glucose-induced insulin exocytosis. *Nature* 402: 685–689, 1999.
28. **Malaisse WJ, Lebrun P, Rasschaert J, Blachier F, Yilmaz T, and Sener A.** Ketone bodies and islet function: ^{86}Rb handling and metabolic data. *Am J Physiol Endocrinol Metab* 259: E123–E130, 1990.
29. **Malaisse WJ, Lebrun P, Yaylali B, Camara J, Valverde I, and Sener A.** Ketone bodies and islet function: ^{45}Ca handling, insulin synthesis, and release. *Am J Physiol Endocrinol Metab* 259: E117–E122, 1990.
30. **Malaisse WJ, Malaisse-Lagae F, and Sener A.** The stimulus-secretion coupling of glucose-induced insulin release: effect of aminooxyacetate upon nutrient-stimulated insulin secretion. *Endocrinology* 111: 392–397, 1982.
31. **Metzger P, Franken P, and Balasse EO.** Permissive role of glucose on the insulinotropic effect of ketone bodies in vivo. *Horm Metab Res* 5: 313–315, 1973.
32. **Patterson GH, Knobel SM, Arkhammar P, Thastrup O, and Piston DW.** Separation of the glucose-stimulated cytoplasmic and mitochondrial NAD(P)H responses in pancreatic islet β cells. *Proc Natl Acad Sci USA* 97: 5203–5207, 2000.
33. **Pralong WF, Spat A, and Wollheim CB.** Dynamic pacing of cell metabolism by intracellular Ca^{2+} transients. *J Biol Chem* 269: 27310–27314, 1994.
34. **Prentki M, Tornheim K, and Corkey BE.** Signal transduction mechanisms in nutrient-induced insulin secretion. *Diabetologia* 40, Suppl 2: S32–S41, 1997.
35. **Proks P, Eliasson L, Ammala C, Rorsman P, and Ashcroft FM.** Ca^{2+}- and GTP-dependent exocytosis in mouse pancreatic β-cells involves both common and distinct steps. *J Physiol* 496: 255–264, 1996.
36. **Rocheleau JV, Head WS, Nicholson WE, Powers AC, and Piston DW.** Pancreatic islet β-cells transiently metabolize pyruvate. *J Biol Chem* 277: 30914–30920, 2002.
37. **Rorsman P.** The pancreatic β-cell as a fuel sensor: an electrophysiologist's viewpoint. *Diabetologia* 40: 487–495, 1997.
38. **Salway JG.** Biosynthesis of ATP 1: ATP, the molecule that powers metabolism. In: *Metabolism at a Glance* (2nd ed.). Malden, MA: Blackwell Science, 1999, p. 12–13.
39. **Salway JG.** Biosynthesis of ATP II: mitochondrial respiratory chain. In: *Metabolism at a Glance* (2nd ed.). Malden, MA: Blackwell Science, 1999, p. 14–15.
40. **Salway JG.** The oxidation of cytosolic NADH: the malate/aspartate shuttle and the glycerol phosphate shuttle. In: *Metabolism at a Glance* (2nd ed.). Malden, MA: Blackwell Science, 1999, p. 16–17.
41. **Schuit F, De Vos A, Farfari S, Moens K, Pipeleers D, Brun T, and Prentki M.** Metabolic fate of glucose in purified islet cells. Glucose-regulated anaplerosis in beta cells. *J Biol Chem* 272: 18572–18579, 1997.
42. **Solomon SS, Ensinck JW, and Williams RH.** Effect of starvation on plasma immunoreactive insulin and non-suppressible insulin-like activity in normal and obese humans. *Metabolism* 17: 528–534, 1968.
43. **Takahashi N, Kadowaki T, Yazaki Y, Ellis-Davies GC, Miyashita Y, and Kasai H.** Post-priming actions of ATP on Ca^{2+}-dependent exocytosis in pancreatic beta cells. *Proc Natl Acad Sci USA* 96: 760–765, 1999.

– 53 –

44. **Tanaka K, Moriya T, Kanamori A, and Yajima Y.** Analysis and a long-term follow up of ketosis-onset Japanese NIDDM patients. *Diabetes Res Clin Pract* 44: 137–146, 1999.

45. **Taniguchi S, Okinaka M, Tanigawa K, and Miwa I.** Difference in mechanism between glyceraldehyde- and glucose-induced insulin secretion from isolated rat pancreatic islets. *J Biochem (Tokyo)* 127: 289–295, 2000.

46. **Vance JE, Buchanan KD, and Williams RH.** Effect of starvation and refeeding on serum immunoreactive glucagon and insulin levels. *J Lab Clin Med* 72: 290–297, 1968.

47. **Zhou YP and Grill V.** Long term exposure to fatty acids and ketones inhibits B-cell functions in human pancreatic islets of Langerhans. *J Clin Endocrinol Metab* 80: 1584–1590, 1995.

– 54 –
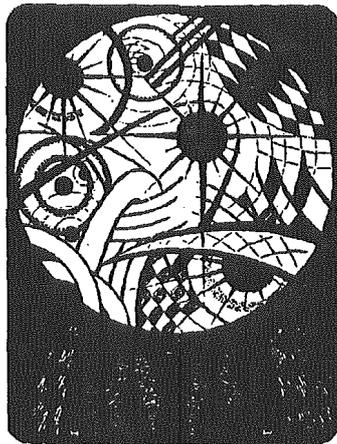
EXPERIMENTAL STUDY

Gastric inhibitory polypeptide is the major insulinotropic factor in K_{ATP} null mice

Katsushi Tsukiyama[1,3], Yuichiro Yamada[1], Kazumasa Miyawaki[1], Akihiro Hamasaki[1], Kazuaki Nagashima[1], Masaya Hosokawa[1], Shimpei Fujimoto[1], Akira Takahashi[1], Kentaro Toyoda[1], Shinya Toyokuni[2], Yutaka Oiso[3] and Yutaka Seino[1]

Departments of [1]Diabetes and Clinical Nutrition and [2]Pathology and Biology of Diseases, Kyoto University Graduate School of Medicine, Kyoto 606-8507, Japan and [3]Department of Endocrinology and Diabetology, Nagoya University Graduate School of Medicine, Nagoya 466-8550, Japan

(Correspondence should be addressed to K Tsukiyama, Department of Diabetes and Clinical Nutrition, Kyoto University Graduate School of Medicine, 54 Shogoin-Kawahara-cho, Sakyo-ku, Kyoto 606-8507, Japan; Email: tukiyama@metab.kuhp.kyoto-u.ac.jp)

Abstract

Objective: ATP-sensitive K^+ (K_{ATP}) channels in pancreatic β-cells are crucial in the regulation of glucose-induced insulin secretion. Recently, K_{ATP} channel-deficient mice were generated by genetic disruption of Kir6.2, the pore-forming component of K_{ATP} channels, but the mice still showed a significant insulin response after oral glucose loading *in vivo*. Gastric inhibitory polypeptide (GIP) is a physiological incretin that stimulates insulin release upon ingestion of nutrients. To determine if GIP is the insulinotropic factor in insulin secretion in K_{ATP} channel-deficient mice, we generated double-knockout Kir6.2 and GIP receptor null mice and compared them with Kir6.2 knockout mice.

Methods: Double-knockout mice were generated by intercrossing Kir6.2-knockout mice with GIP receptor-knockout mice. An oral glucose tolerance test, insulin tolerance test and batch incubation study of pancreatic islets were performed on double-knockout mice and Kir6.2-knockout mice.

Results: Fasting glucose and insulin levels were similar in both groups. After oral glucose loading, blood glucose levels of double-knockout mice became elevated compared with Kir6.2-knockout mice, especially at 15 min (345 ± 10 mg/dl vs 294 ± 20 mg/dl, $P < 0.05$) and 30 min (453 ± 20 mg/dl vs 381 ± 26 mg/dl, $P < 0.05$). The insulin response was almost completely lost in double-knockout mice, although insulin secretion from isolated islets was stimulated by another incretin, glucagon-like peptide-1 in the double-knockout mice. Double-knockout mice and Kir6.2-knockout mice were similarly insulin sensitive as assessed by the insulin tolerance test.

Conclusion: GIP is the major insulinotropic factor in the secretion of insulin in response to glucose load in K_{ATP} channel-deficient mice.

European Journal of Endocrinology 151 407–412

Introduction

The regulation of glucose-induced insulin secretion depends critically on glucose metabolism in pancreatic β-cells, and electrical activity controlled by plasma membrane ion channels is especially important (1). The ATP–sensitive K^+ (K_{ATP}) channel links glucose metabolism to membrane potentials (2–4). ATP closes the K_{ATP} channels, which activates voltage-dependent calcium channels, initiating insulin release.

Recently, K_{ATP} channel-deficient mice were generated by genetic disruption of Kir6.2, which forms the K^+ ion-selective pore of the channel (5). While there is no increment in insulin secretion in response to high glucose concentration *in vitro* in Kir6.2-knockout (Kir6.2$^{-/-}$) mice, as assessed by perifusion and batch incubation of isolated pancreatic islets, the mice still show the insulin response after oral glucose loading *in vivo*.

Insulinotropic hormones secreted from the gut upon nutritional ingestion play an important role in glucose-induced insulin secretion (6, 7). Gastric inhibitory polypeptide (GIP) is released from duodenal and upper small intestinal endocrine K-cells upon absorption of glucose or fat (8), and potentiates insulin secretion from pancreatic β-cells by binding to its specific receptor, the GIP receptor (GIPR). This incretin stimulates adenylyl cyclase, raises cyclic AMP (cAMP), and activates protein kinase A or type-II isoform of cAMP-regulated guanine nucleotide exchange factor (cAMP-GEF II) (9). We previously generated mice with a targeted disruption of the GIPR gene (10). Islets from GIPR-knockout

(GIPR$^{-/-}$) mice respond to glucose as well as wild-type mice, but GIPR$^{-/-}$ mice exhibit higher blood glucose levels and an impaired initial insulin response after oral glucose loading.

In the present study, we have generated double-knockout Kir6.2 and GIPR null (Kir6.2$^{-/-}$GIPR$^{-/-}$) mice, and have found that Kir6.2$^{-/-}$GIPR$^{-/-}$ mice lack the insulin response to oral glucose load seen in Kir6.2$^{-/-}$ mice, clearly indicating that GIP is the major insulinotropic factor in the insulin secretory activity in these mice.

Design and methods

Generation of animal models

Kir6.2$^{-/-}$ mice were provided by T Miki and S Seino, Chiba University Graduate School of Medicine, Japan. GIPR$^{-/-}$ mice were generated as described previously (10). Kir6.2$^{+/-}$GIPR$^{+/-}$ mice were generated by intercrossing Kir6.2$^{-/-}$ mice with GIPR$^{-/-}$ mice. Crossbreeding of Kir6.2$^{+/-}$GIPR$^{+/-}$ mice yielded Kir6.2$^{-/-}$GIPR$^{-/-}$ mice. All animals received care in accordance with the principles of laboratory animal care adopted by Kyoto University and the Declaration of Helsinki.

Batch incubation study

Pancreatic islets were isolated from 18- to 19-week-old male mice by collagenase digestion, and batch incubation was performed as described previously (11), with slight modification. Briefly, pancreatic islets (10 in each tube) were preincubated at 37 °C for 60 min in Hepes-Krebs buffer containing 118.4 mmol/l NaCl, 4.7 mmol/l KCl, 1.2 mmol/l KH$_2$PO$_4$, 2.4 mmol/l CaCl$_2$, 1.2 mmol/l MgSO$_4$, 20 mmol/l NaHCO$_3$, 2.8 mmol/l glucose, and 10 mmol/l Hepes, supplemented with 0.2% (wt/vol) BSA. The islets were incubated for 30 min in 400 μl buffer containing various stimuli of insulin secretion. GIP and glucagon-like peptide-1 (GLP-1) were obtained from Peptide Institute, Inc., Osaka, Japan. Tolbutamide was from Nacalai Tesque Inc., Kyoto, Japan.

Immunohistochemical analysis

The pancreata of 18-week-old male mice were removed and fixed in Bouin's solution. Pancreatic specimens were embedded in paraffin and sectioned at 3.5 μm. The avidin–biotin complex method with alkaline phosphatase was used as previously described (12), with a slight modification. After deparaffinization, normal goat serum (diluted to 1:75) (DAKO, Kyoto, Japan) for inhibition of nonspecific binding of primary antibody, rabbit anti-insulin antibody (diluted to 1:350) (DAKO) or rabbit anti-glucagon antibody (OAL-123, kindly provided by Otsuka Assay Laboratory, Tokushima, Japan)

(13) in a final dilution of 1:500, the biotin-labeled goat anti-rabbit IgG antibody (diluted to 1:300) (DAKO), and avidin-biotin-alkaline phosphatase complex (diluted to 1:100) (Vector Laboratories, Burlingame, CA, USA) were sequentially applied on sections, followed by hematoxylin nuclear counterstaining. Staining was visualized in red and black by alkaline phosphatase substrate (Vector Laboratories) for insulin and glucagon respectively. The sections were analyzed using the NIH Image software (http://rsb.info.nih.gov/nih-image/), and the area containing insulin-positive β-cells was calculated.

Measurements of blood glucose and insulin levels

An oral glucose tolerance test (OGTT) was performed on age-matched male mice at 10 to 11 weeks of age. After a 16-h fast, plasma insulin and blood glucose levels were measured and glucose (2 g/kg body weight) was loaded orally. In the insulin tolerance test, 0.1 unit/kg body weight of human insulin (Eli Lilly, Indianapolis, IN, USA) was injected subcutaneously in male mice (17 weeks of age) after a 16-h fast. Blood samples were taken from the tail vein at the times indicated. Blood glucose levels were measured by an enzyme-electrode method in whole blood. Plasma insulin levels were determined by a high-sensitive ELISA kit (Shibayagi, Gunma, Japan).

Glucose uptake in jejunum in vitro

Incorporation of D-glucose into everted jejunal rings was determined as described previously (14), with slight modifications. Briefly, mice were anesthetized with pentobarbital sodium (60 mg/kg s.c.) and a segment of jejunum was quickly excised, rinsed with saline solution (140 mmol/l NaCl, 10 mmol/l KHCO$_3$, 0.4 mmol/l KH$_2$PO$_4$, 2.4 mmol/l K$_2$HPO$_4$, 1.2 mmol/l CaCl$_2$ and 1.2 mmol/l MgCl$_2$, pH 7.4), everted, and cut into ~30 mg pieces. Groups of 4 intestinal rings were incubated for 15 min at 37 °C and continuously gassed with O$_2$ in buffer containing 1.0 mmol/l D-glucose and 0.1 μCi/10 ml D-[^{14}C]glucose (specific activity 50–60 mCi/mmol; Amersham Radiochemical Center, London, UK) in the absence and presence of 1 mmol/l phlorizin (phloretin 2′-glucoside), a potent inhibitor of Na$^+$/glucose cotransporter (SGLT). At the end of the incubation period, the tissues were washed in ice-cold saline solution twice, blotted carefully to remove excess moisture, weighed, and extracted by shaking for 24 h in 1 ml 100 mmol/l HNO$_3$ (at 4 °C). An aliquot was taken and radioactivity was determined by liquid scintillation counting on a Liquid Scintillation Analyzer (model TRI-CARB 1900CA, Packard Instrument Company Inc., Downers Grove, IL, USA). SGLT-dependent glucose uptake was determined as the glucose uptake

in the absence of phlorizin minus the glucose uptake in the presence of phlorizin.

Results

Insulin secretion in isolated islets

Insulin secretory responses of Kir6.2$^{-/-}$GIPR$^{-/-}$ mice were examined *in vitro* by batch incubation study. Total
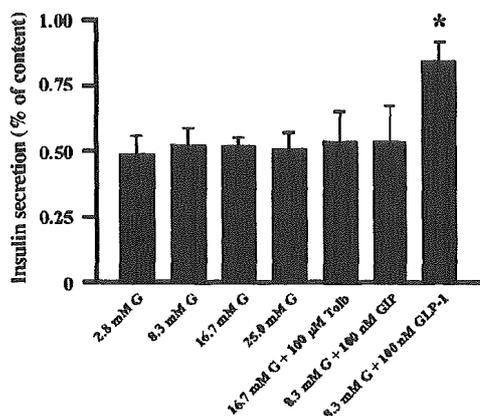
Figure 1 Insulin secretion from islets of Kir6.2$^{-/-}$GIPR$^{-/-}$ mice. Insulin secretion in batch-incubated pancreatic islets of Kir6.2$^{-/-}$ GIPR$^{-/-}$ mice in response to the indicated concentrations of glucose (G), 100 μmol/l tolbutamide (Tolb), 100 nmol/l GIP and 100 nmol/l GLP-1 are shown. Values are means±s.e.m., relative to the insulin content in averaged single islets of Kir6.2$^{-/-}$ GIPR$^{-/-}$ mice (n = 40). *P < 0.05 compared with 2.8 mmol/l glucose.

insulin content per single islet is decreased in Kir6.2$^{-/-}$ GIPR$^{-/-}$ mice compared with wild-type (Kir6.2$^{+/+}$ GIPR$^{+/+}$) mice (47.3±3.5%, data not shown). In comparison with the basal level of insulin secretion at 2.8 mmol/l glucose from batch-incubated pancreatic islets, the insulin secretion in Kir6.2$^{-/-}$ GIPR$^{-/-}$ mice in response to 8.3 mmol/l glucose, 16.7 mmol/l glucose, 25.0 mmol/l glucose, 100 μmol/l tolbutamide in the presence of 16.7 mmol/l glucose or 100 nmol/l GIP in the presence of 8.3 mmol/l glucose is similar. In contrast, 100 nmol/l GLP-1 in the presence of 8.3 mmol/l glucose elicits an increased response (Fig. 1).

Immunohistochemistry of pancreatic islets

Immunohistochemical examination shows that the number of insulin-positive β-cells in islets of Kir6.2$^{-/-}$ GIPR$^{-/-}$ is increased, and that the area containing insulin-positive cells in the islets of Kir6.2$^{-/-}$GIPR$^{-/-}$ mice is increased by 32.6% compared with Kir6.2$^{-/-}$ GIPR$^{+/+}$ mice. Glucagon-positive α-cells, which are present primarily in the periphery in islets of Kir6.2$^{+/+}$ GIPR$^{+/+}$ mice, also appear in the central region in islets of Kir6.2$^{-/-}$GIPR$^{-/-}$ mice, as in Kir6.2$^{-/-}$ GIPR$^{+/+}$ mice (Fig. 2).

Glucose tolerance and insulin secretion in vivo

Fasting glucose levels are similar in Kir6.2$^{-/-}$ GIPR$^{-/-}$, Kir6.2$^{-/-}$GIPR$^{+/+}$, and Kir6.2$^{+/+}$GIPR$^{+/+}$ mice. However, after oral glucose loading, blood glucose
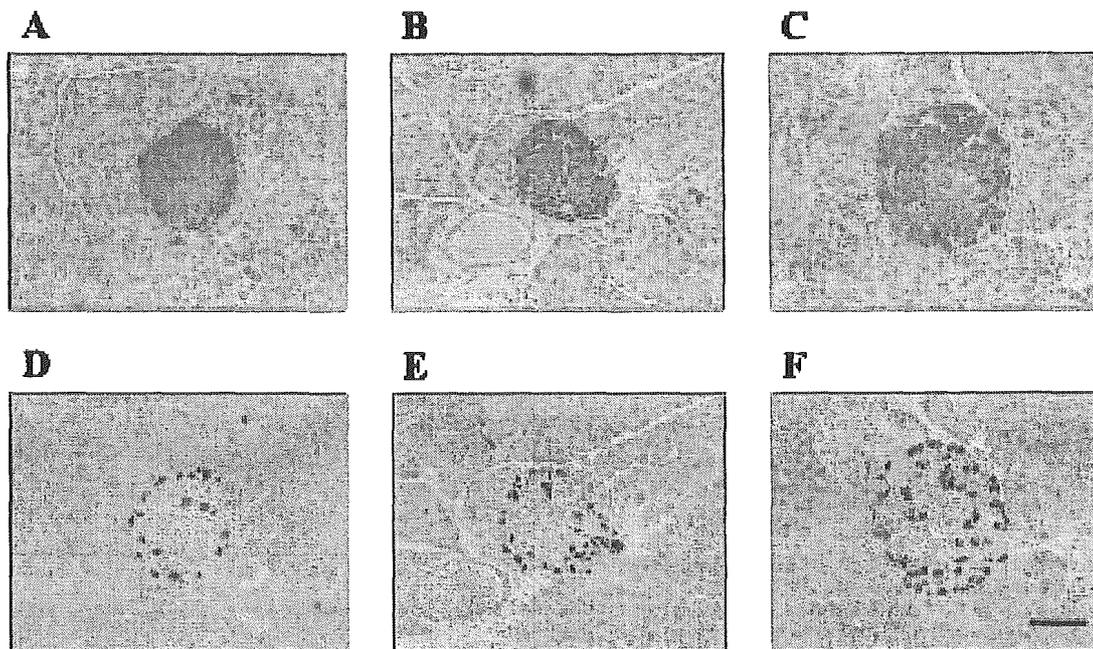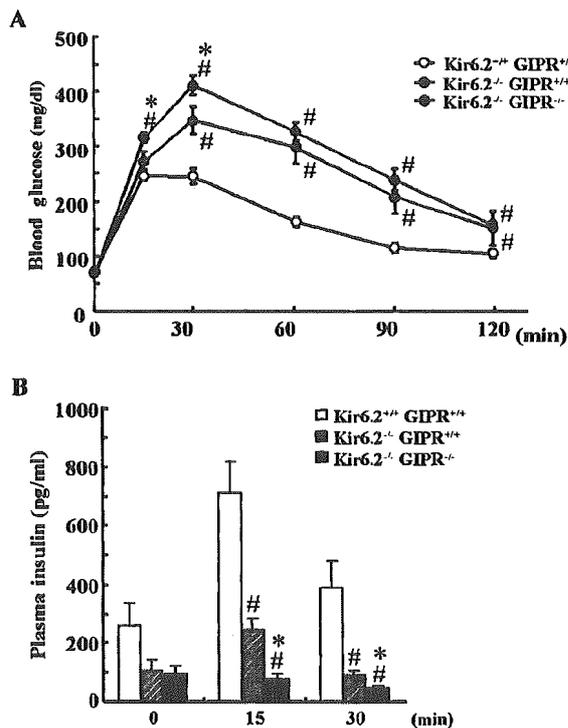

Figure 2 Immunohistochemical analyses of pancreatic islets. Immunohistochemical analyses of pancreatic islets of Kir6.2$^{+/+}$GIPR$^{+/+}$ mice (A, D), Kir6.2$^{-/-}$GIPR$^{+/+}$ mice (B, E), and Kir6.2$^{-/-}$GIPR$^{-/-}$ mice (C, F) are shown. Pancreatic β-cells and α-cells were stained using rabbit anti-insulin antibodies (A, B and C) or anti-glucagon antibodies (D, E and F). Bar = 100 μm.

levels of $Kir6.2^{-/-}GIPR^{-/-}$ mice become elevated compared with $Kir6.2^{-/-}GIPR^{+/+}$ mice, especially at 15 min (345 ± 10 mg/dl vs 294 ± 20 mg/dl, $P < 0.05$) and 30 min (453 ± 20 mg/dl vs 381 ± 26 mg/dl, $P < 0.05$) (Fig. 3A). The time of peak glucose response is at 30 min both in $Kir6.2^{-/-}GIPR^{-/-}$ mice and $Kir6.2^{-/-}GIPR^{+/+}$ mice. Plasma insulin levels were measured to determine the cause of the glucose intolerance in $Kir6.2^{-/-}GIPR^{-/-}$ mice. Fasting insulin levels in $Kir6.2^{-/-}GIPR^{-/-}$ mice and $Kir6.2^{-/-}GIPR^{+/+}$ mice are similar. The insulin response after oral glucose loading is almost completely lost in $Kir6.2^{-/-}GIPR^{-/-}$ mice, and the insulin levels at 15 min and 30 min in $Kir6.2^{-/-}GIPR^{-/-}$ mice are lower than in $Kir6.2^{-/-}GIPR^{+/+}$ mice (Fig. 3B), indicating that the glucose intolerance in $Kir6.2^{-/-}GIPR^{-/-}$ mice is due to insufficient insulin secretion.

Glucose uptake by the jejunum in vitro

We investigated glucose uptake by the jejunum *in vitro* using everted jejunal rings, and found no difference among $Kir6.2^{+/+}GIPR^{+/+}$, $Kir6.2^{-/-}GIPR^{+/+}$ and $Kir6.2^{-/-}GIPR^{-/-}$ mice (Fig. 4).

Insulin sensitivity in vivo

The glucose-lowering effect of insulin was assessed by an insulin tolerance test. $Kir6.2^{-/-}GIPR^{-/-}$ mice and $Kir6.2^{-/-}GIPR^{+/+}$ mice are similarly insulin sensitive, and more so than $Kir6.2^{+/+}GIPR^{+/+}$ mice (Fig. 5).

Discussion

GIP and GLP-1 are physiological incretins (7, 15) that stimulate insulin secretion from pancreatic β-cells upon ingestion of nutrients. GIP and GLP-1 bind to specific receptors, the GIPR and the GLP-1 receptor (GLP-1R), and increase the intracellular cAMP concentration, which produces insulin secretion. However, functional differences have become clear in recent studies of knockout mice (10, 16–18). $GIPR^{-/-}$ mice exhibit normal glucose tolerance after intraperitoneal glucose loading but impaired glucose tolerance after oral glucose loading, while GLP-1R-knockout ($GLP-1^{-/-}$) mice exhibit impaired glucose tolerance

Figure 4 Glucose uptake in the jejunum. Glucose uptake in the jejunum in $Kir6.2^{+/+}GIPR^{+/+}$ mice, open bar; $Kir6.2^{-/-}GIPR^{+/+}$ mice, hatched bar; $Kir6.2^{-/-}GIPR^{-/-}$ mice, solid bar is shown ($n = 4$). Na^+/glucose cotransporter (SGLT)-dependent glucose uptake was determined as the glucose uptake in the absence of phlorizin minus the glucose uptake in the presence of 1 mmol/l phlorizin. Values are means $\pm$ S.E.M.
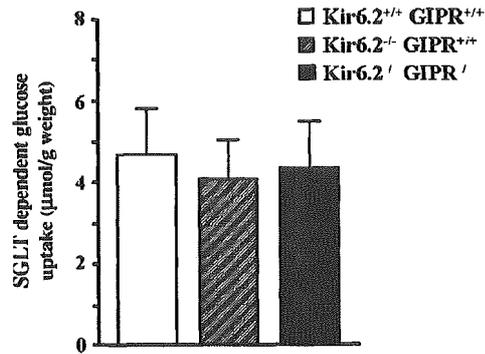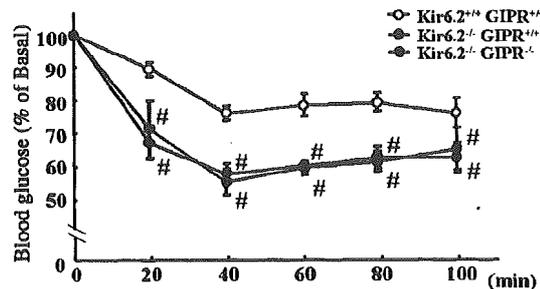
Figure 3 Glucose tolerance test. (A) Blood glucose levels after oral glucose loading are shown: $Kir6.2^{+/+}GIPR^{+/+}$ mice, open circles; $Kir6.2^{-/-}GIPR^{+/+}$ mice, hatched circles; $Kir6.2^{-/-}GIPR^{-/-}$ mice, solid circles ($n = 5$). (B) Plasma insulin levels after oral glucose tolerance test are shown: $Kir6.2^{+/+}GIPR^{+/+}$ mice, open bars; $Kir6.2^{-/-}GIPR^{+/+}$ mice, hatched bars; $Kir6.2^{-/-}GIPR^{-/-}$ mice, solid bars ($n = 5$). Values are means $\pm$ S.E.M. $\#P < 0.05$ vs $Kir6.2^{+/+}GIPR^{+/+}$ mice; $*P < 0.05$ vs $Kir6.2^{-/-}GIPR^{+/+}$ mice.

Figure 5 Insulin tolerance test. Changes in blood glucose levels upon insulin injection are shown: $Kir6.2^{+/+}GIPR^{+/+}$ mice, open circles; $Kir6.2^{-/-}GIPR^{+/+}$ mice, hatched circles; $Kir6.2^{-/-}GIPR^{-/-}$ mice, solid circles ($n = 5$). Values are means $\pm$ S.E.M., relative to basal blood glucose levels. $\#P < 0.05$ compared with $Kir6.2^{+/+}GIPR^{+/+}$ mice.